

Zeitschrift: Schweizerische mineralogische und petrographische Mitteilungen =
Bulletin suisse de minéralogie et pétrographie

Band: 80 (2000)

Heft: 2

Artikel: High-precision dating and origin of synsedimentary volcanism in the
Late Carboniferous Salvan-Dorénaz basin (Aiguilles-Rouges Massif,
Western Alps)

Autor: Capuzzo, Nicola / Bussy, François

DOI: <https://doi.org/10.5169/seals-60958>

Nutzungsbedingungen

Die ETH-Bibliothek ist die Anbieterin der digitalisierten Zeitschriften. Sie besitzt keine Urheberrechte an den Zeitschriften und ist nicht verantwortlich für deren Inhalte. Die Rechte liegen in der Regel bei den Herausgebern beziehungsweise den externen Rechteinhabern. [Siehe Rechtliche Hinweise.](#)

Conditions d'utilisation

L'ETH Library est le fournisseur des revues numérisées. Elle ne détient aucun droit d'auteur sur les revues et n'est pas responsable de leur contenu. En règle générale, les droits sont détenus par les éditeurs ou les détenteurs de droits externes. [Voir Informations légales.](#)

Terms of use

The ETH Library is the provider of the digitised journals. It does not own any copyrights to the journals and is not responsible for their content. The rights usually lie with the publishers or the external rights holders. [See Legal notice.](#)

Download PDF: 22.01.2025

ETH-Bibliothek Zürich, E-Periodica, <https://www.e-periodica.ch>

Dedicated to Prof. Dr. Martin Frey on the occasion of his 60th birthday

High-precision dating and origin of synsedimentary volcanism in the Late Carboniferous Salvan-Dorénaz basin (Aiguilles-Rouges Massif, Western Alps)

by Nicola Capuzzo¹ and François Bussy^{2,3}

Abstract

Late Variscan volcanic activity is documented in the Late Carboniferous Salvan-Dorénaz sedimentary basin and in the neighboring basement units of the Aiguilles-Rouges and Mont-Blanc crystalline massifs (Western Alps). Precise U/Pb isotopic dating, zircon morphology and geochemical analyses indicate that volcanism occurred during short-lived pulses and that coexisting crustal and mantle sources were involved in the production of melts. Volcanic and subvolcanic products were emplaced along major N–S to NNE–SSW transtensional fracture zones, similar to the ones that governed intense basement exhumation and that favored the formation and filling of the Late Carboniferous Salvan-Dorénaz continental basin.

In the Aiguilles-Rouges massif, dacitic flows outcropping at the base of the Salvan-Dorénaz basin erupted at 308 ± 3 Ma; they represent the surface equivalent of the nearby Vallorcine peraluminous granite and associated rhyolitic dykes (311 ± 17 Ma). In the Mont-Blanc massif, calc-alkaline rhyolitic dykes were emplaced simultaneously (307 ± 2 Ma) at shallow crustal levels, but they derive from deeper magma sources denoting enhanced mantellic activity.

Recently identified tuffs and volcanoclastic layers embedded at different levels of the Salvan-Dorénaz stratigraphic record testify a $295 +3/-4$ Ma old episode of highly explosive volcanism from distant volcanic centers, possibly located in the Aar-Gotthard massifs (Central Alps). Their zircon typology is highly heterogeneous, documenting wall-rock contamination of the melts and/or admixture of crustal sediments, whereas consistent subpopulations point to high-temperature magmas of deep-seated origin and alkaline affinity.

The dated volcanic layers from the Salvan-Dorénaz basin set the beginning of the detrital sedimentation at 308 ± 3 Ma and constrain the deposition of 1.5–1.7 km thick of clastic sediments within a time span of 10–15 Ma. These results infer minimum, long-term subsidence rates during basin evolution in the order of > 0.1 mm/a, while in the surrounding basement units estimated exhumation rates are in the range of 1 mm/a. All dated rocks contain inherited zircon populations about 350, 450 or 600 Ma old.

Keywords: Late Variscan volcanism, volcano-sedimentary basin, zircon geochronology, Aiguilles-Rouges massif and Mont-Blanc massif.

Introduction

The Variscan orogeny resulted from the Late Palaeozoic multiple and oblique continental collisions between Gondwana and Gondwana-derived microplates to the south and Laurasia to the north. Collision and accretion of Gondwana-derived terranes in the Moldanubian Zone, a tectonometamorphic unit of the internal orogenic root domain, led to a thickened continental crust

and a Barrowian-type metamorphism culminating in Mid-Carboniferous time (MATTE, 1991; VON RAUMER, 1998). The reorganization of the regional stress field during the Late Carboniferous led to the development of crustal-scale dextral strike-slip zones in the consolidated part of the Variscides (ARTHAUD and MATTE, 1977; ZIEGLER, 1990; HENK, 1999), where post-orogenic readjustment processes of the thickened crust took place (e.g., BURG et al., 1994, and reference therein). As a

¹ Geologisch-Paläontologisches Institut, Universität Basel, Bernoullistrasse 32, CH-4056 Basel, Switzerland. <Nicola.Capuzzo@unibas.ch>

² Institut de Minéralogie et Pétrographie, Université de Lausanne, BFSH 2, CH-1015 Lausanne, Switzerland. <Francois.Bussy@imp.unil.ch>

³ Geochronology Laboratory, Royal Ontario Museum, 100, Queen's Park, Toronto, Ontario, Canada, M5S 2C6.

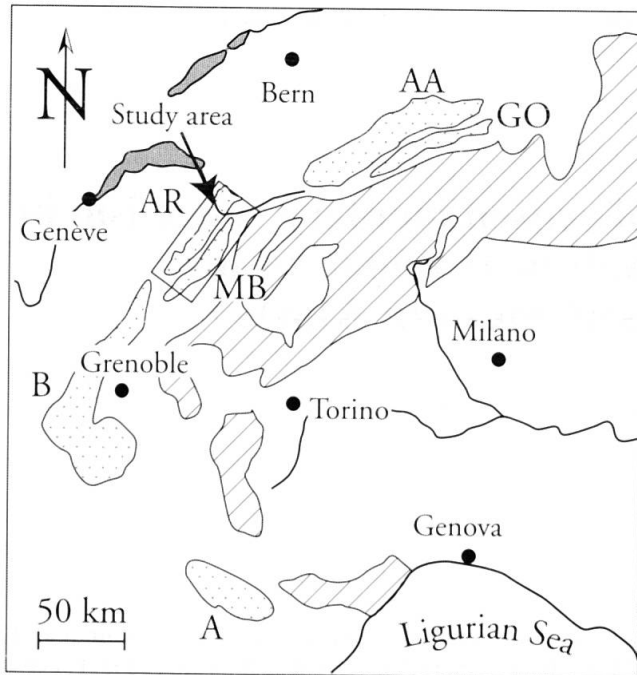


Fig. 1 Pre-Mesozoic basement rocks in the Alps (shaded) and External Alpine Crystalline Massifs (stippled). AA: Aar; Go: Gotthard; AR: Aiguilles-Rouges; MB: Mont-Blanc; B: Belledonne; A: Argentera (modified after SCHALTEGGER and CORFU, 1995).

consequence numerous strike-slip and pull-apart basins formed in central and southern Europe with concomitant exhumation of metamorphic core complexes and widespread magmatism (ZIEGLER, 1993; CASSINIS *et al.*, 1992; KRAINER, 1993).

The main characteristics of the Variscan post-collisional evolution are: (a) regional uplift with erosional processes that reached mid-crustal levels; (b) localized areas of intense tectonic subsidence filled with thick clastic continental series, which rest unconformably on high-grade crystalline rocks (VON RAUMER, 1998); and (c) widespread intrusive and extrusive magmatism of mantle and crustal derivation (BONIN *et al.*, 1993; BENEK *et al.*, 1996; CORTESOGNO *et al.*, 1998; BUSSY *et al.*, 2000). In many places active volcanism accompanied continental sedimentation and it occurred along transtensional to extensional structures. Late Carboniferous to Early Permian basins containing varying amounts of volcanites are described in the Northeast German basin (BENEK *et al.*, 1996), in the Saar-Nahe basin (SCHÄFER, 1989; STOLLHOFEN and STAINSTREET, 1994), in the northern Permocarboniferous Swiss troughs (MATTER, 1987; SCHALTEGGER, 1997a), in the Alpine External Crystalline massifs (Fig. 1; Aar massif, FRANKS, 1968; SCHALTEGGER and CORFU, 1995; Aiguilles-Rouges massifs, CAPUZZO and BUSSY, 2000; Grandes Rousses, BANZET *et al.*,

1985), and in the Ligurian and Southern Alps (CORTESOGNO *et al.*, 1998, and references therein).

The present study focuses on the Salvan-Dorénaz basin, a Late Carboniferous continental basin exposed with a NNE–SSW direction along the eastern margin of the Aiguilles-Rouges massif (Fig. 2). It formed as an intra-continental, fault bounded, sedimentary trough during transtensive and strike-slip tectonics and it contains different types of continental facies deposited in a rapidly subsiding basin. Stratigraphically, the age of the basin fill was determined by macroflora associations indicating Upper Westphalian and Stephanian ages (JONGMANS, 1960; WEIL, 1999). Unfortunately, the low stratigraphical resolution of paleoflora associations around the Carboniferous–Permian boundary of western Europe does not allow a precise stratigraphical determination since mixed associations often occur (BROUTIN *et al.*, 1986; BECO-GIRAUDON, 1993; and references therein). In addition, the presence of thick series of reddish coarse-grained sediments has often been interpreted as evidence of Permian sedimentation (OULIANOFF, 1924; SUBLET, 1962).

Volcanic rocks occur along the western base of the Salvan-Dorénaz basin (SUBLET, 1962; PILLOUD, 1991) and, more recently, tuffs and volcanoclastic layers were also identified at different levels of the basin fill (NIKLAUS and WETZEL, 1996; CAPUZZO and BUSSY, 2000).

As volcanic layers are excellent potential geochronological markers and occur throughout the Salvan-Dorénaz stratigraphic record, a systematic U–Pb zircon dating coupled to zircon typology and geochemistry was carried out to determine:

- the exact time frame of continental sedimentation;
- the average subsidence rates during basin evolution;
- the presence or not of Permian deposits;
- possible sources of the synsedimentary volcanic products;
- their links to magmatic pulses documented in the nearby Aiguilles-Rouges and Mont-Blanc basement units.

Regional geological setting

The Aiguilles-Rouges and the nearby Mont-Blanc massifs are part of the so-called External Crystalline massifs of the French and Swiss Alps and they represent basement nappes or slices appearing as Alpine antiformal cores among their Mesozoic covers. The External Crystalline massifs belong to the former Moldanubian internal zone of the Variscan belt (VON RAUMER *et al.*, 1993)

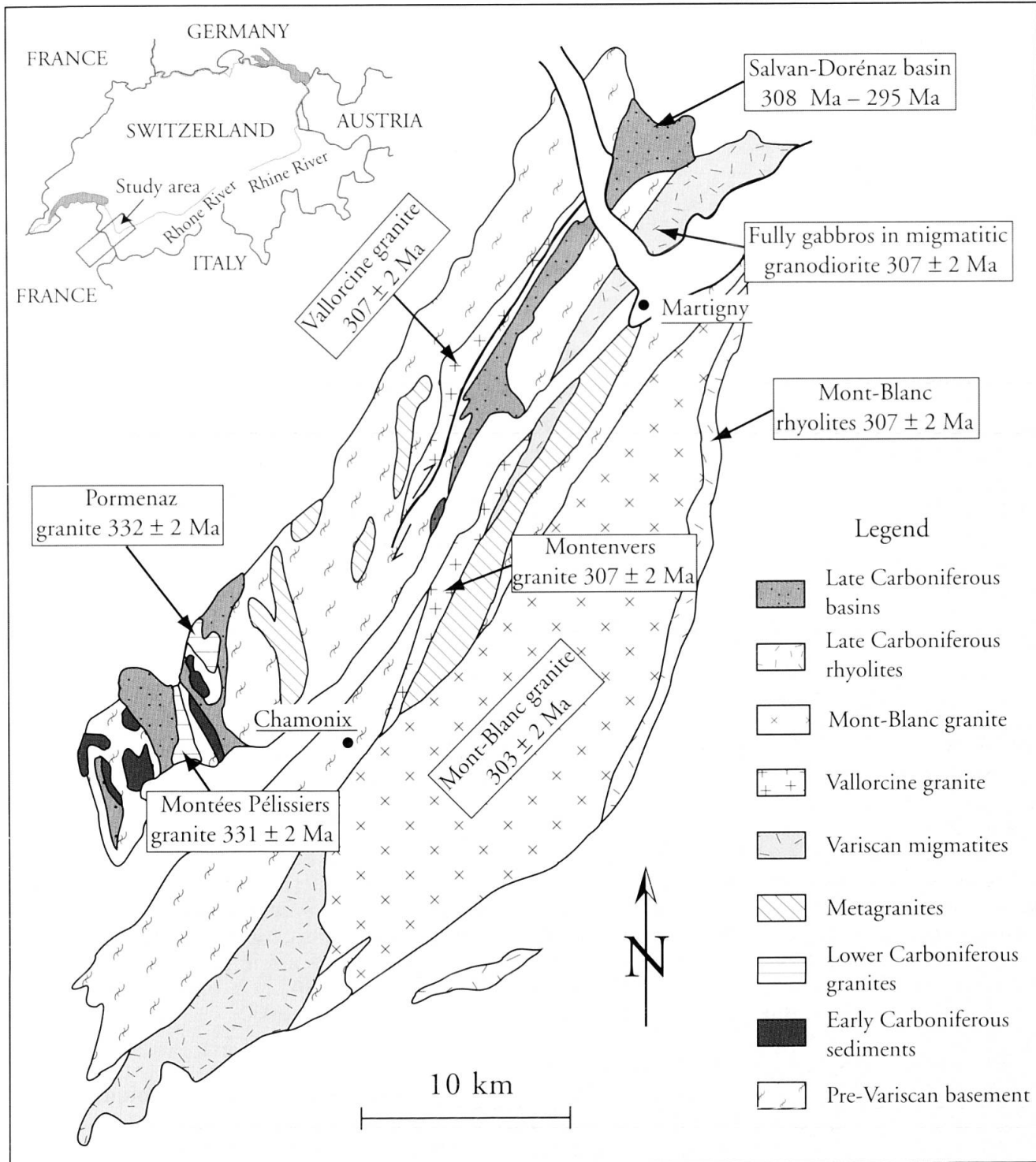


Fig. 2 Geographical location, in upper left, and geological map of the Aiguilles-Rouges and Mont-Blanc massifs (modified after BRÄNDLEIN et al., 1994). The two massifs are formed by metamorphic and magmatic basement rocks and secondly by Carboniferous detrital sediments containing various amounts of volcanites. They appear as nappes in Alpine antiform cores among their Mesozoic cover. U/Pb ages are from this study and after BUSSY et al. (2000).

and preserve most of their late orogenic, essentially Carboniferous evolution. The Tertiary Alpine overprint reached only the lowermost greenschist facies in the Aiguilles-Rouges and a slightly higher grade in the nearby Mont-Blanc massif (VON RAUMER, 1971; FREY et al., 1999).

The Aiguilles-Rouges massif consists of a complex assemblage of tectonic units with contrasting maximum P-T metamorphic conditions and separated by major, steeply dipping N-S faults and/or mylonitic zones (VON RAUMER et al., 1999). It is essentially composed of Palaeozoic

polymetamorphic, amphibolite-facies grade rocks and granitic plutons (Fig. 2). The Mont-Blanc massif is similar to the Aiguilles-Rouges massif, from which it was ca. 20 km apart before the Alpine orogeny (EPARD, pers. comm.). It differs in its slightly deeper structural units and stronger Alpine deformation.

Age determinations in the External Crystalline massifs indicate a polyorogenic evolution, comprising Variscan, Ordovician and Late Precambrian events (VON RAUMER 1998; VON RAUMER et al., 1999). The earliest record of the Variscan collision in the Aiguilles-Rouges/Mont-Blanc area is probably documented by the Lake Cornu eclogites (700 °C / min. 14 kbar; SCHULZ and VON RAUMER, 1993). On the other hand, paragneisses experienced a succession of deformation events related to early thrust tectonics (DOBMEIER, 1998) and nappe stacking, with development of a Barrowian-type metamorphism (VON RAUMER et al., 1999) documenting cooling ages between 327–316 Ma (DOBMEIER et al., 1999). Metapelites record a typical clockwise P-T path, as commonly found in the internal parts of the Variscides (e.g. REY et al., 1997). Relics of high-P kyanite-bearing parageneses were overprinted by high-T sillimanite-bearing mineral assemblages dated at 327 ± 2 Ma (U–Pb age on monazite, BUSSY et al., 2000). Subsequent isothermal pressure drop, ascribed to fast tectonic exhumation, triggered *in situ* decompression melting, dated at 320 ± 1 Ma and 317 ± 2 Ma on Aiguilles-Rouges and Mont-Blanc leucosomes, respectively (BUSSY and VON RAUMER, 1993; BUSSY et al., 2000). In the meantime (since at least 330 Ma), the initial thrust tectonic regime switched to a long-lasting, transcurrent regime with dextral sense of shear along subvertical N–S to NNE–SSW fault zones, such as those delimiting the western flank of the Salvan-Dorénaz basin (SCHULZ and VON RAUMER, 1993; BUSSY et al., 2000).

The Variscan magmatic activity in the External Crystalline massifs consists of short-lived pulses (e.g. BUSSY and HERNANDEZ, 1997; SCHALTEGGER, 1997b; DEBON and LEMMET, 1999; BUSSY et al., 2000). In the Aiguilles-Rouges and Mont-Blanc area, a first pulse at ca. 330 Ma is documented by the syntectonic intrusion along major transpressive faults of the mantle-derived Pormenaz monzonite (BUSSY et al., 1997), and the crust-derived Montées-Pélessier peraluminous granite (BUSSY et al., 2000) (Fig. 2). A second pulse occurred at 307 ± 2 Ma with syntectonic intrusion along dextral transtensional shear zones of the high-T cordierite-bearing granites of Vallorcine (BRÄNDLEIN et al., 1994) and Montenvers (MORARD, 1998), as well as the Fully anatectic granodiorite (BOVAY, 1988). The latter hosts co-

eval gabbro enclaves, again documenting a mantle contribution. Finally, the large Mont-Blanc ferriferous granite and coeval mafic rocks (BUSSY, 1990) intruded at 303 ± 2 Ma (BUSSY and VON RAUMER, 1993). Its alkali-calcic nature is consistent with the general tendency of the late Variscan magmatism to evolve towards increasingly alkaline post-orogenic series (BONIN et al., 1998; BUSSY et al., 2000). Subvolcanic facies occur both in the Aiguilles-Rouges and Mont-Blanc massifs as granite-porphyry and rhyolite dykes.

Carboniferous volcano-sedimentary deposits are known within the Aiguilles-Rouges basement units. Low-grade detrital sediments of Viséan age with intercalated calc-alkaline volcanites occur at the southern end of the massif (DOBMEIER, 1996; DOBMEIER et al., 1999); whereas Late Carboniferous anchizonal sediments crop-out in the Pormenaz and Salvan-Dorénaz Alpine synclines (Fig. 2). In the latter a total thickness of 1.5–1.7 km of sediments accumulated within four different lithological units in response to intrabasinal differential subsidence and tectonic movements (NIKLAUS and WETZEL, 1996; CAPUZZO et al., 1997). They are schematically reported in the geological map and relative cross-sections of the northern areas of the basin (Figs 3a, b). Active volcanism occurred during its initial development as shown by subaerial flows and autobreccia deposits outcropping along its north-western base (SUBLET, 1962; PILLOUD, 1991), and by several rhyolitic and ignimbritic pebbles embedded in the lower depositional unit (Figs 3a, b; CAPUZZO and BUSSY, 2000). In addition, recently identified tuffs and volcanoclastic layers outcropping in the upper levels of the basin testify for intense, high explosive, synsedimentary volcanism possibly derived from distant sources (NIKLAUS and WETZEL, 1996; CAPUZZO and BUSSY, 2000).

Samples and analytical techniques

The investigated samples mainly consist in volcanic and volcanogenic deposits outcropping at different levels of the Salvan-Dorénaz basin. A few samples of subvolcanic and plutonic rocks from the neighboring Aiguilles-Rouges and Mont-Blanc basement units were also analyzed for comparison (for sample description and location, see annex 1). A synthetic description of the field and petrographical features of these lithologies is given in the next section.

Five samples from volcanic and volcanoclastic rocks in the Salvan-Dorénaz basin and from subvolcanic dykes in the Aiguilles-Rouges and Mont-Blanc massifs were selected for U/Pb geochronol-

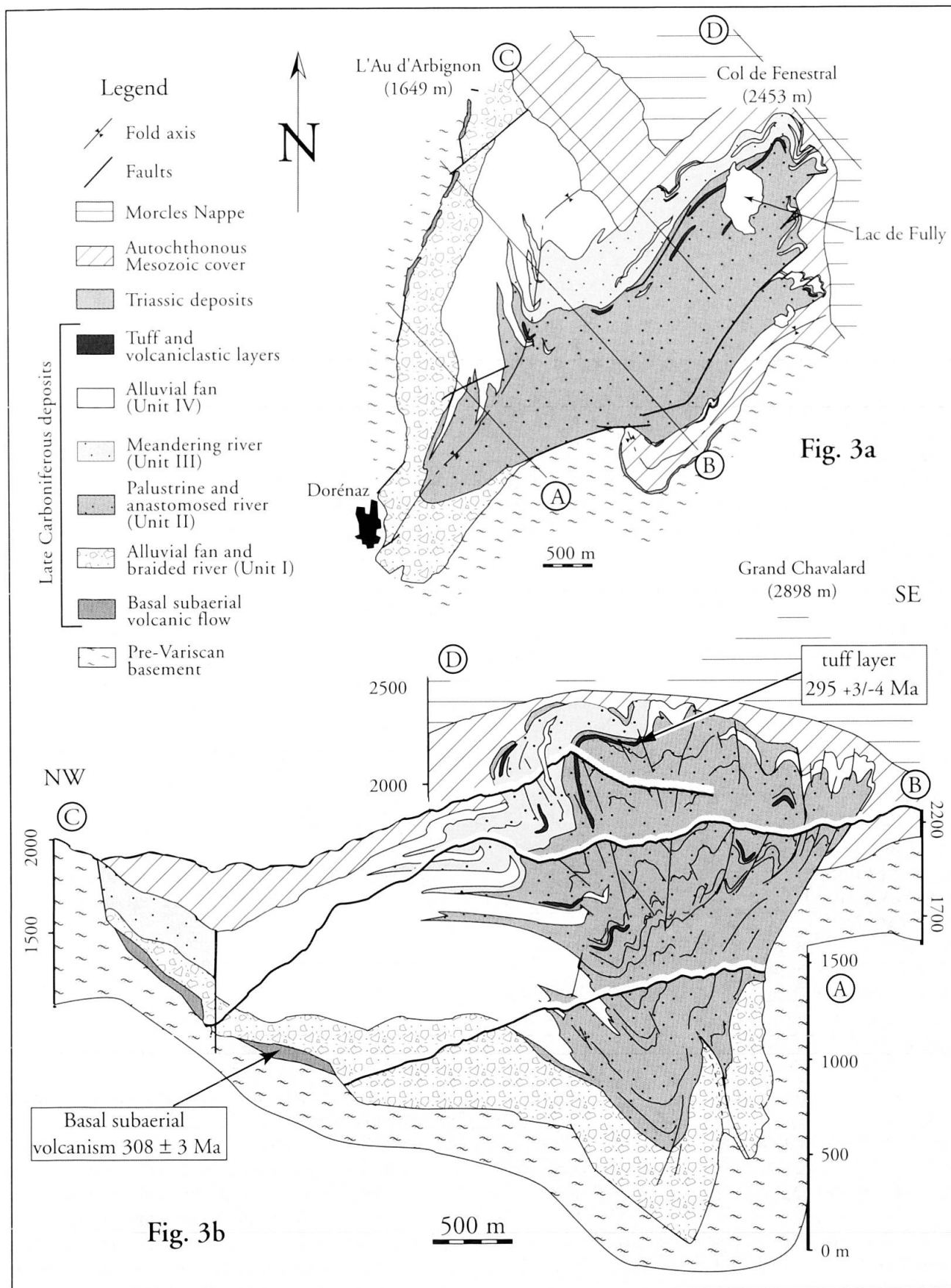


Fig. 3 (a) Geological map of the northern areas of the Salvan-Dorénaiz syncline. The four lithological units that fill the basin are schematically reported, as the location of the volcanic and volcanigenic layers. (b) Multiple cross-sections of the northern areas of the Salvan-Dorénaiz syncline. Section lines are reported in the geological map and indicated by capital letters (modified after PILLOUD, 1991).

ogy on zircons. The U–Pb dating of zircons (Tab. 1) was done using the conventional isotope dilution technique at the Royal Ontario Museum of Toronto, Canada. Zircons were extracted from 20–25 kg of fresh material, using classical heavy liquid and magnetic separation techniques. The analyzed crystals were selected according to criteria detailed in BUSSY and CADOPPI (1996). Zircons with smoothed edges were systematically rejected to minimize the risk of analyzing reworked or xenocryst grains. Chemistry and measurements were made following the standard procedure of KROGH (1973). Air-abrasion was applied systematically to eliminate surface-correlated lead loss and younger overgrowths (KROGH, 1982). Regression lines were computed using the ISO-PLOT/EX program of LUDWIG (1999). All errors are quoted at the 95% confidence level.

Whole rock major and trace element concentrations were measured by X-ray fluorescence spectrometry (XRF) (Philips PW 1400 equipment) at the Centre d'Analyse Minérale of the University of Lausanne on 13 samples principally selected among new founding of volcanic and volcanogenic deposits in the Salvan-Dorénaz basin. Data are reported in table 2. Seven samples were processed for Rare Earth Element analyses (REE). Data, reported in table 3, were obtained by inductively coupled plasma mass spectrometry (ICP-MS) (VG-PQ2) at the Laboratoire de Géodynamique des Chaînes Alpines of the University of Grenoble following the procedure of BARRAT et al. (1996). Sm and Nd isotopes were isolated on the same samples by ion exchange chromatography at Grenoble as well, whereas Nd isotopic measurements were performed on a multi-collector ICP-MS (Nu Instrument) at the University of Bern (Tab. 4).

The main mineral phases of the fine-grained tuff and volcanoclastic layers were determined by powder X-ray diffraction analysis (Siemens D-5000 X-ray diffractometer) at the Geochemical Laboratory of the University of Basel.

Field data and petrography

BASAL SUBAERIAL VOLCANISM

The volcanic flows outcropping at the base of the Salvan-Dorénaz trough are characterized by variable proportions of coherent and autoclastic scoriaceous volcanic facies interlayered toward the top with Upper Carboniferous sediments. They present porphyritic textures with large euhedral and subhedral quartz and plagioclase pheno-

crysts. The latter were mostly replaced by albite during subsequent retrogression. Quartz frequently shows perlitic fractures and typical resorption features. Subsidiary altered biotite flakes and a few K-feldspars are dispersed in the microcrystalline matrix. Accessory minerals such as garnet, apatite, zircon and opaque minerals also occur. Coarse-grained garnets are interpreted as xenocrysts from crumbling wall rocks, incorporated during the ascent of magma. Fine-grained quartz reaction rims document chemical disequilibrium between garnets and the melt. Both pheno- and xenocrysts are frequently cracked as a result of shear during flow and/or pressure release during rise and eruption of the magma.

VOLCANIC PEBBLES

Rounded volcanic pebbles, petrographically similar to the basal volcanic deposits, occur within conglomeratic beds outcropping in the Salvan-Dorénaz basin. Samples described here were collected in the lower stratigraphical levels of the Late Carboniferous sediments. They show eutaxitic texture with different welded pumice fragments and devitrified glass shards. Quartz and plagioclase phenocrysts are frequently aligned along flow direction. Coarse-grained garnet xenocrysts also occur. All these features are typical for ignimbritic flows. They were probably erupted in the source areas of detrital material, subsequently eroded, and transported via alluvial fan systems into the Salvan-Dorénaz basin. Their tectonically undeformed fabric and petrographic characteristics suggest a close relation to the local magmatic pulse recorded at the base of the Salvan-Dorénaz basin.

TUFF LAYERS

Fine to very fine-grained tuffs (ash-fall deposits) ranging in thickness from 5 to 70 cm and showing lateral continuity, mantle bedding, delicate planar laminations and fining-upward tendency are interlayered in the upper levels of the Late Carboniferous sediments. They consist of a fine-grained matrix containing dispersed chloritized glass shards, few fragmented quartz and plagioclase crystals, biotite flakes, and opaque and heavy minerals. The cryptocrystalline matrix is intensely silicified and some secondary carbonate patches may occur in it. The main mineral phases determined with powder X-ray diffraction analyses are: quartz, albite, illite and clinocllore.

VOLCANICLASTIC LAYERS

Several volcaniclastic sandstones were found in the upper levels of the Salvan-Dorénaz basin. They consist of mixed volcaniclastic and detrital grains and sometimes show well developed cross-stratification indicating reworking by traction currents. They range in thickness from 50 to 160 cm and are intimately interlayered with siltstone and sandstone beds. Their fabric is matrix- to grain-supported. The clastic components are mainly derived from volcanic sources. Broken devitrified glass shards, monocristalline quartz and plagioclase fragments, and biotite flakes indicate a volcanic origin. On the other hand, micaschist and high-grade metamorphic clasts, polycristalline quartz, intensely altered K-feldspars and white mica flakes point toward detrital sources.

SUBVOLCANIC DYKES IN THE AIGUILLES-ROUGES AND MONT-BLANC BASEMENT UNITS

In the Aiguilles-Rouges, subvolcanic facies occur as granite-porphry and rhyolite vertical dykes, which crosscut both the Vallorcine granite and its country rocks (BRÄNDLEIN *et al.*, 1994; LERESCHE, 1992). They might represent feeding dykes of the basal volcanism preserved in the Salvan-Dorénaz basin. They show injection structures with locally well developed chilled margins, and complete transition from porphyritic to microcrystalline to spherulitic textures (LERESCHE, 1992; BRÄNDLEIN *et al.*, 1994). Quartz phenocrysts are frequently rounded and corroded; idiomorphic to hypidiomorphic plagioclases are intensely replaced by albite and sericite. Micas are uncommon and intensely altered. Accessory minerals such as garnet, apatite, zircon, rutile and opaques also occur. Flowage microstructures around the phenocrysts are well preserved with no sign of intense deformation or recrystallization (BRÄNDLEIN *et al.*, 1994).

A complex network of shallow-level dykes and a subvolcanic rhyolite stock a few km² wide (MARRO, 1986) occur along the eastern side of the Mont-Blanc massif (Fig. 2), probably emplaced during periods of subaerial fissure volcanism favored by NE to NNE trending fracture zones (BURRI and MARRO, 1993). These rhyolites display porphyritic to microcrystalline textures, with rare to abundant plagioclase, K-feldspar and resorbed quartz phenocrysts up to 5 mm long. The fine-grained matrix is composed of microcrystalline quartz with occasional fluidal textures, which partially recrystallized during Alpine metamorphism (BURRI and MARRO, 1993).

Zircon typology and geochronology

Nine samples of lava flows and tuff layers from the Salvan-Dorénaz basin have been processed for zircon extraction. Among them, six did not contain this mineral at all (e.g. CN256 and CN257) or only rounded grains (e.g. CN 108 and CN113), suggesting either a sedimentary derivation with abrasion during transport and/or a xenocrystic origin with dissolution within the host magma. In both cases, these resorbed grains could not provide reliable ages of syndepositional volcanic activity and therefore were not further considered. All three remaining samples (CN118, CN125 and CN140) contained at least some sharp faceted zircon crystals, which have been preferentially selected for U-Pb dating (Tab. 1). In addition, zircons were also extracted from two samples of subvolcanic dykes from the Aiguilles-Rouges and Mont-Blanc massifs.

SUBAERIAL BASAL FLOW (CN125)

This sample essentially contains variously resorbed stubby zircons with smoothed edges suggesting a xenocryst origin. By contrast, a secondary zircon population consists of sharp faceted acicular prisms and needle crystals. From a morphological point of view, there is no significant difference between the two sub-populations. The {211} pyramid is largely dominant over the {101} one (mean A index = 281); whereas the {110} prism is moderately more developed than the {100} one (mean T index = 415) (Fig. 4). According to PUPIN (1980; 1988), this kind of zircon is typical of intrusive granitic magmas of crustal anatexic origin (Fig. 5). Its relatively high mean T index points to rather high-temperature melts, above the incongruent melting point of biotite at the source. If part of the zircons is indeed of xenocryst origin, the contaminant material should itself be peraluminous in composition.

Four small zircon fractions have been selected for U-Pb dating (Tab. 1). To avoid inherited cores, only needles and hollow flat prisms have been considered in fractions [8] to [11], whereas 3 stubby prisms have been selected for fraction [12]. The results yield a rather complicated pattern (Fig. 6); fractions [8], [11] and [12] are all three concordant ([12] not shown in Fig. 6), but at contrasting ages of 347, 308 and 440 Ma, respectively. This age heterogeneity confirms that several zircon populations are mixed together, as inferred by the morphological features. The youngest age of 308 ± 3 Ma yielded by [11] is interpreted as dating the magmatic growth of zircons within the dacitic

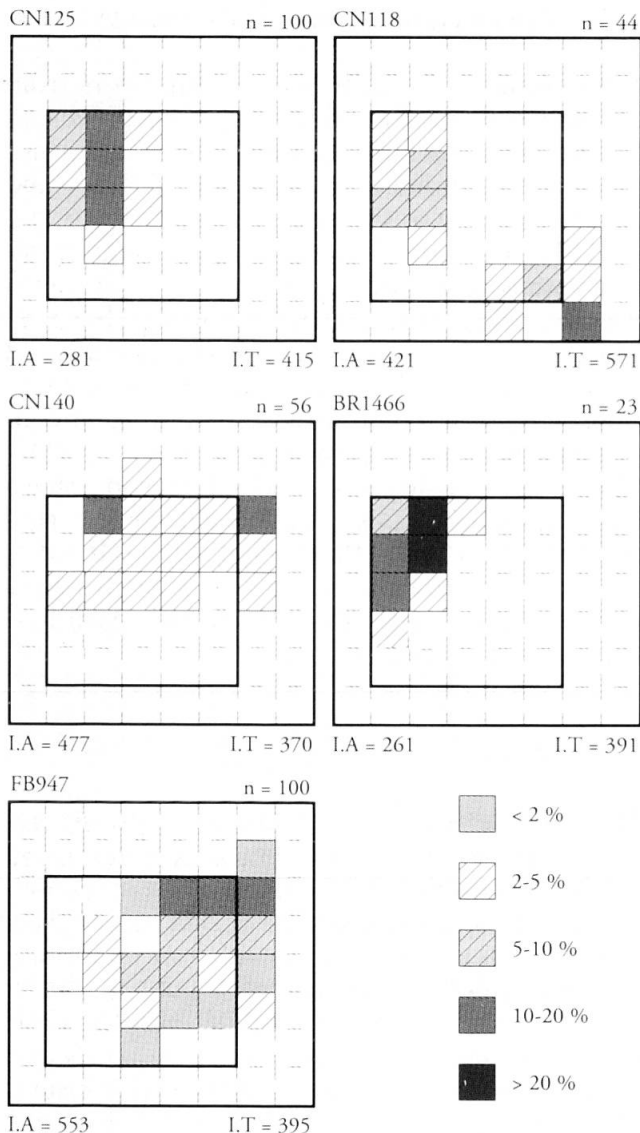


Fig. 4 Zircon morphology distribution in the typologic classification of PUPIN (1980) for volcanic and subvolcanic rocks from the Aiguilles-Rouges and Mont-Blanc massifs. For description and provenance of samples, see text and annex 1. n = number of analysed zircons; I.A. and I.T. = mean A and T indices, respectively.

melt, which fed the basal lava flow. On the other hand, zircons from fractions [8] to [10] represent another population about 350 Ma old, as they plot linearly in the Concordia diagram, defining an upper intercept age of 349 ± 7 Ma. These zircons are interpreted as xenocrysts incorporated into the dacitic melt at the source or during the ascent of magma. The same is true for the 440 Ma old zircons of fraction [12].

TUFF LAYER CN118

This rock-type is characterized by low concentrations of tiny and euhedral zircons, which define two well-contrasted morphological populations

(Fig. 4). The first one consists of stubby bipyramidal prisms with well-developed {211} facets, typical of peraluminous melts. Some of these crystals are slightly resorbed (smoothed outlines). The second population is characterized by acicular, sharp faceted prisms with poorly developed or absent {211} and {110} crystallographic forms, which indicate very high A (> 600) and T (> 700) indices. These features are specific to alkali-calcic and alkaline acidic melts (Fig. 5). Such contrasting zircon populations cannot grow in the same magma and thus clearly document mixing processes. Considering the resorbed outline of some of the low A index zircons and their mid-crustal anatectic origin, it is inferred that they have been incorporated as xenocrysts into an alkaline magma, whereas the high A index zircons crystallized directly in the melt.

On this basis, only high A index zircons were selected for U-Pb isotopic dating. Seven single-grain or small multi-grain fractions were analyzed (fractions [1] to [7], Tab. 1). All plot concordantly between 290 and 297 Ma within analytical errors, which are rather large for the single-grain loads (fractions [1] to [3]) (Fig. 6). Relying preferentially on the $^{206}\text{Pb}/^{238}\text{U}$ and $^{207}\text{Pb}/^{235}\text{U}$ ages of the most concordant data points, we propose an age of $295 \pm 3/4$ Ma for the volcanic ash production and deposition.

VOLCANICLASTIC SANDSTONE (CN140)

This horizon was selected since it outcrops in the uppermost preserved part of the stratigraphic record of the Salvan-Dorénaz basin. It contains numerous zircons, mostly ovoid in shape, but sometimes acicular and sharp faceted. Their morphological distribution is bipolar, although less clearly than for sample CN118. Zircons present a large range of A indices, with maxima at A = 300 and 700, respectively (Fig. 4). This pattern can be interpreted in two different ways: it might either correspond to the evolution of a peraluminous magma, with early low-A index morphologies evolving towards high-A index ones, as often seen in the differentiated acidic magmas (PUPIN, 1980); or it could be a situation similar to that observed in CN118, with an alkaline acidic magma crystallizing high-A index zircons, and incorporating low-A index xenocrystic zircons during its evolution. The latter population could have also been supplied by the clastic input of this volcano-sedimentary rock.

Three small zircon fractions were selected for U-Pb dating (fractions [13] to [15], Tab. 1). Considering the high probability of inheritance, usual-

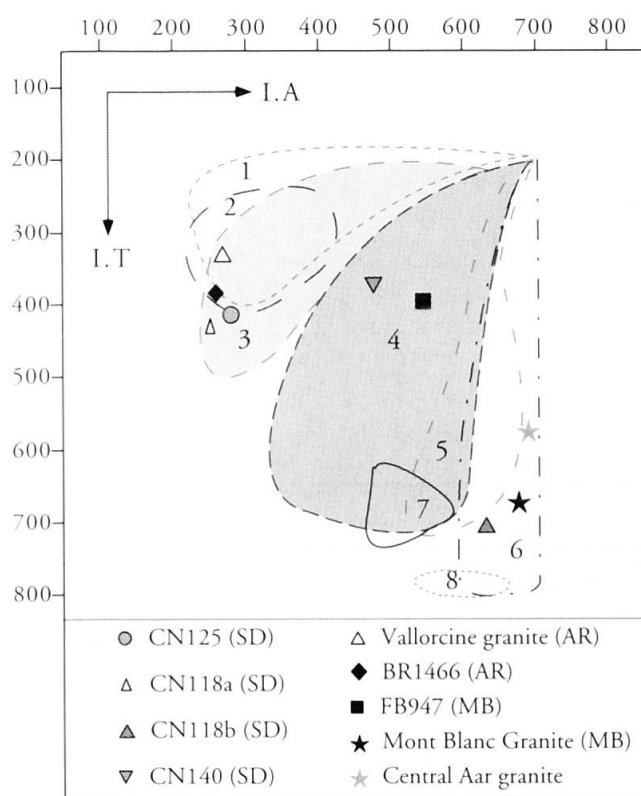


Fig. 5 Distribution of the mean A/T points of the analysed volcanic and subvolcanic samples in the classification diagram of PUPIN (1988).

(1) aluminous granites; (2) sub-autochthonous monzogranites-granodiorites; (3) intrusive aluminous monzogranites-granodiorites; (4) calc-alkaline and K-calc-alkaline series granites; (5) sub-alkaline series granites; (6) alkaline series granites; (7) continental tholeiitic granites; (8) oceanic tholeiitic series granites.

The distribution pattern points to a bimodal Late Carboniferous magmatism in the Aiguilles-Rouges and Mont-Blanc massifs. Data for Vallorcine, Mont-Blanc and Central Aar granites are from BONIN et al. (1993). Samples number and location reported in annex 1.

ly associated to low-A index zircons, only sharp faceted acicular prisms or needles were selected. The three fractions are collinear in the Concordia diagram, which documents a common crystallization age of ca. 440 Ma, well constrained by the concordant fraction [15] (Fig. 6). The CN140 volcanoclastic horizon thus hosts a large and well preserved inherited zircon population of Silurian age. No evidence for Carboniferous zircons has been found; they probably have a stubby morphology, which has been dismissed during the selection procedure.

AIGUILLES-ROUGES RHYOLITIC DYKE (BR1466)

Red rhyolitic dykes, ca. 2–3 m thick and 1200 m long, outcrop in the Salanfe area (Aiguilles-Rou-

ges massif) and are classically considered as Permian in the literature (BRÄNDLEIN, 1991; BRÄNDLEIN et al., 1994). Since they crosscut all tectonic structures of the country rocks, their dating yields an upper time limit for the ductile deformation in the Aiguilles-Rouges massif. The processed sample contains very few zircons, either acicular and cloudy, with many bubbles and melt inclusions, or more stubby with ovoid outlines. Because of the very small number of crystals available, only 23 grains were morphologically characterized. They all have low A and T indices (mean A and T indices = 261 and 391, respectively; Fig. 4), typical of aluminous anatectic melts (Fig. 5).

Seven zircon fractions were analyzed (Tab. 1, fractions [20] to [26]). Fractions [22] and [23] are concordant within large analytical uncertainties (Fig. 6), due to their very small amount of radiogenic Pb, at $^{206}\text{Pb}/^{238}\text{U}$ ages of 289 and 293 Ma, respectively. Fraction [24] is slightly discordant at a $^{206}\text{Pb}/^{238}\text{U}$ age of 305 Ma. On the other hand, fraction [21] is 25% discordant at a younger U–Pb age pointing to episodic lead loss, whereas fractions [20], [25] and [26] are discordant at higher apparent ages, evidencing the presence of Lower Paleozoic inherited cores. The available data do not allow a precise age determination, which should lie close to 300 Ma, in any case below 307 ± 2 Ma, as the dyke crosscuts the Vallorcine granite. Nevertheless, a minimum age for the dyke intrusion can be calculated on the basis of the collinear fractions [21] to [23]. If the lower intercept of the discordia line is tightened to 0 ± 30 Ma (assuming Alpine lead loss), the upper intercept age is 311 ± 17 Ma, which defines a minimum intrusion age of 294 Ma for this rhyolitic dyke.

MONT-BLANC RHYOLITE (FB947)

This greenish sub-volcanic rock contains numerous euhedral pinkish zircons, rich in bubbles and melt inclusions. Their morphological distribution (Fig. 4) is bipolar, with a dominant population characterized by high A indices of 600–700 (the {211} pyramid is subordinate or even absent), as are zircons from the neighboring Mont-Blanc alkali-calcic granite (Fig. 5). A subsidiary zircon population has noticeably lower A indices between 300 and 400. The latter can hardly crystallize in the same magma as the dominant high-A index zircons and are considered as resulting from source and/or wall-rock contamination.

Four rather large zircon fractions have been selected for U–Pb isotopic dating (Tab. 1, fractions [16] to [19]). Fractions [18] and [19] consisted of colorless needles and are perfectly concor-

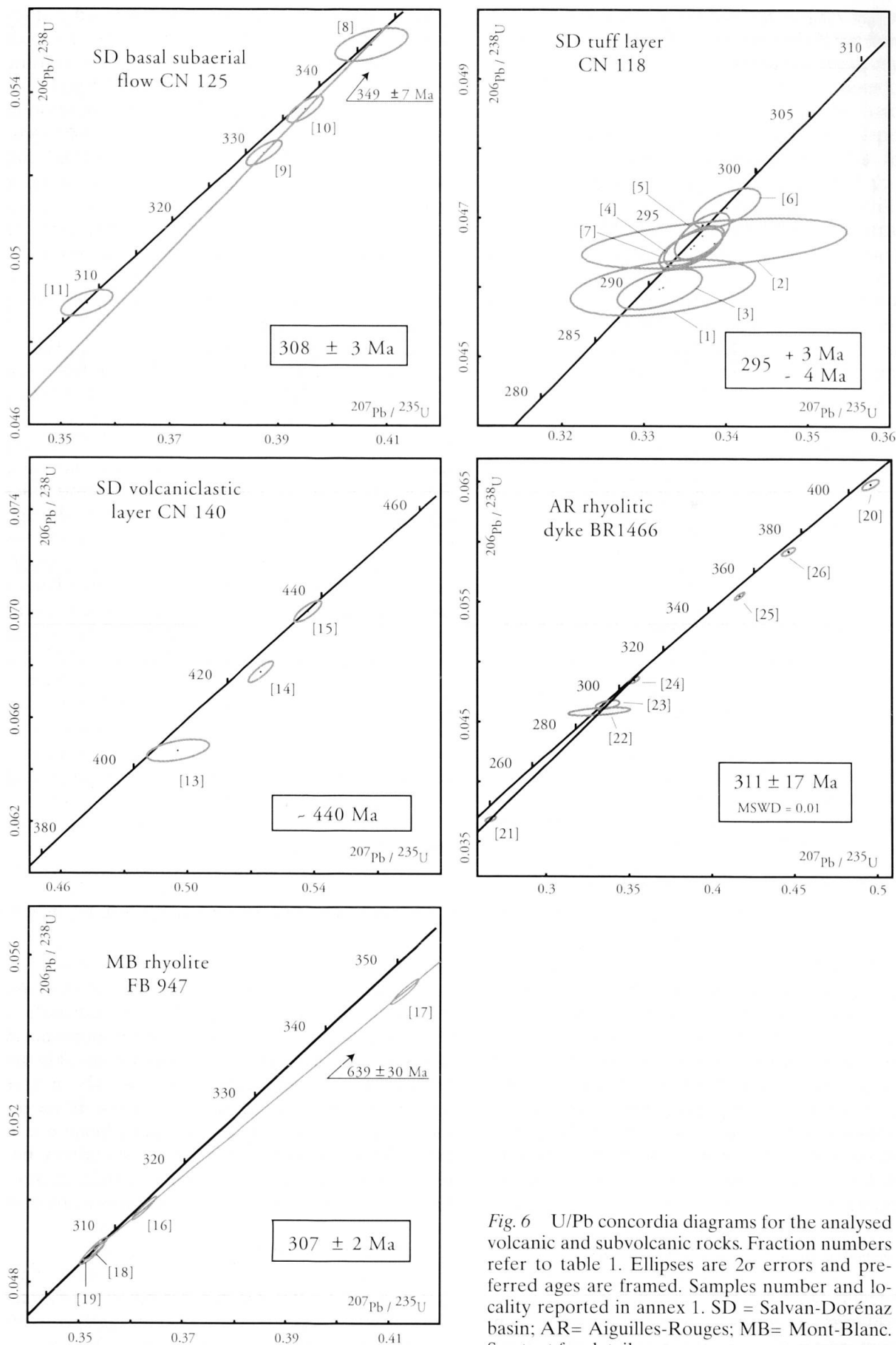


Fig. 6 U/Pb concordia diagrams for the analysed volcanic and subvolcanic rocks. Fraction numbers refer to table 1. Ellipses are 2σ errors and preferred ages are framed. Samples number and locality reported in annex 1. SD = Salvan-Dorénaz basin; AR= Aiguilles-Rouges; MB= Mont-Blanc. See text for details.

dant at 307 ± 2 Ma, whereas [16] and [17] yield older apparent ages (Fig. 6). A discordia line drawn through all points gives an upper intercept age of 639 ± 30 Ma (MSWD = 0.77), documenting a Pan-African inherited component. Relying on the concordant data, a magmatic age of 307 ± 2 Ma is proposed for the Mont-Blanc rhyolite. Considering both zircon ages and typologies, these rhyolites seem unrelated to any volcanic products outcropping in the Salvan-DorénaZ basin.

Geochemistry

NOMENCLATURE

Considering the sedimentary environment into which most of the analysed samples were deposited, intense chemical modifications due to weathering and/or diagenesis are to be expected. Furthermore, differentiation processes related to the fall-out deposition of ashes, as well as input of detrital material have partially modified the original chemical composition of the tuff and volcanoclastic layers. Depletion in Na_2O and CaO and relative enrichment in K_2O and Al_2O_3 were considered as chemical indication of intense weathering

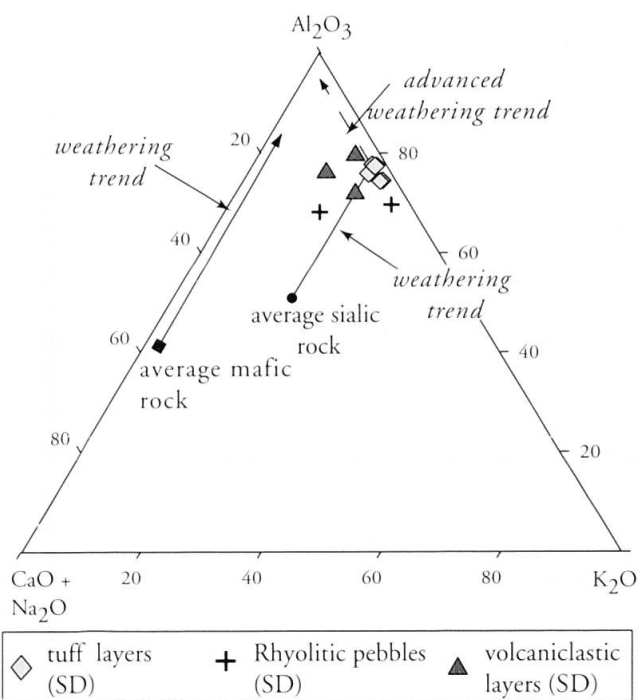


Fig. 7 Diagram of weathering trends for silicic and mafic magmatic rocks (after NESBITT and YOUNG, 1984; 1989). The tuff and volcanoclastic layers as well as the volcanic pebbles occurring in the Salvan-DorénaZ basin (SD) show major elements chemical modification possibly related to intense weathering. Data reported in table 2.

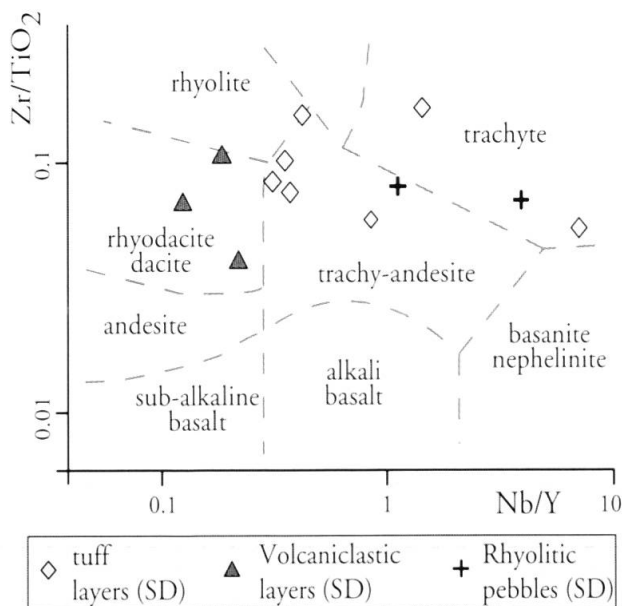


Fig. 8 Nb/Y vs Zr/TiO_2 classification diagram (WINCHESTER and FLOYD, 1977) for the tuffs, volcanoclastic layers and volcanic pebbles occurring in the Salvan-DorénaZ basin (SD). Data reported in table 2. See text for discussion.

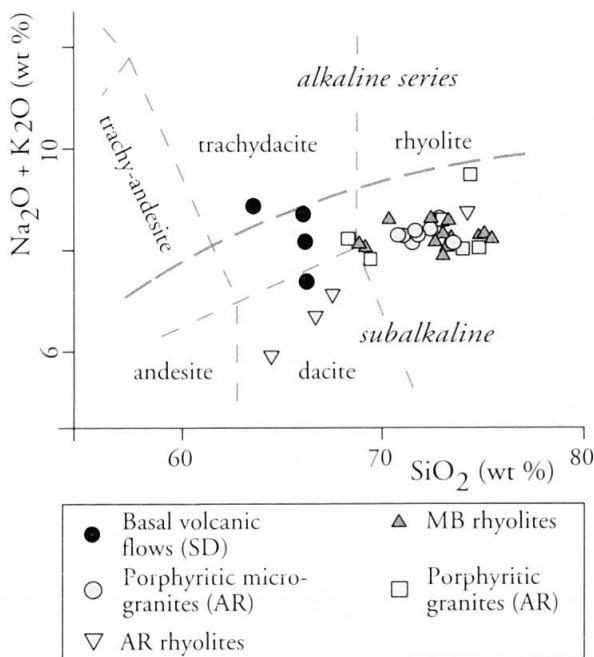


Fig. 9 TAS classification diagram (LE MAITRE et al., 1989) for the Late Carboniferous volcanic flows at the base of the Salvan-DorénaZ basin and for subvolcanic rocks in the Aiguilles-Rouges (AR) and Mont-Blanc (MB) massifs. Subdivision between alkaline and sub-alkaline series after IRVINE and BARAGAR (1971). New data are reported in table 2. Data compared from the literature are those of: PILLOUD (1991) for the basal dacitic flows; BRÄNDLEIN (1991), BRÄNDLEIN et al. (1994) and LERESCHE (1992) for the Aiguilles-Rouges subvolcanic dykes; MARRO (1986) and BURRI and MARRO (1993) for the Mont-Blanc rhyolites.

Tab. 1 U/Pb analyses of zircons extracted from volcanic and volcanogenic deposits in the Salvan-Dorénaz basin (SD) and from subvolcanic dykes in the Aiguilles-Rouges (AR) and Mont-Blanc (MB) massifs. See text for description and annex 1 for location of samples.

Sample (fraction N° and grain characteristics)	Mass		Concentrations			Atomic ratios			Apparent ages (Ma)			
	mg	U	Pb*	208Pb*	Th/U	206/204	206/238	207/235	207/206	6/38	7/35	7/6
CN118 – tuff layer (SD)												
1 single hollow needle	0.001	164	8	10	0.37	340	0.04600±34	0.3323±46	0.0524±13	289.9	291.4	303.1
2 single flat hollow prism	0.001	139	7	12	0.45	196	0.04664±30	0.3386±132	0.0527±19	293.8	296.1	314.2
3 single acicular prism	0.001	423	19	7	0.25	708	0.04597±24	0.3319±42	0.05236±56	289.7	291.0	301.2
4 4 hollow grains	0.003	211	10	6	0.21	1136	0.04660±24	0.3361±36	0.05231±36	293.6	294.2	299.0
5 7 hollow fragments	0.003	302	14	10	0.35	1424	0.04674±28	0.3371±28	0.05231±34	294.5	295.0	299.0
6 8 fragments	0.003	214	10	7	0.24	1046	0.04714±24	0.3401±34	0.05233±42	297.0	297.3	299.8
7 9 fragments	0.003	231	11	10	0.34	1500	0.04656±24	0.3357±32	0.05230±38	293.4	293.9	298.5
CN125 – subaerial basal flow (SD)												
8 2 needles	0.001	345	18	5	0.18	853	0.05517±32	0.4072±54	0.05353±60	346.2	346.8	351.1
9 5 small needles	0.001	877	44	5	0.18	2136	0.05256±24	0.3874±26	0.05346±24	330.2	332.5	348.4
10 3 flat hollow prisms	0.002	482	25	5	0.17	2324	0.05361±26	0.3950±28	0.05344±24	336.7	338.0	347.5
11 2 elongated prisms	0.001	597	28	5	0.17	934	0.04894±26	0.3548±40	0.05257±48	308.0	308.3	310.5
12 3 short prisms	0.001	711	48	6	0.20	2195	0.07005±38	0.5385±48	0.05575±36	436.5	437.4	442.5
CN140 – volcanoclastic layer (SD)												
13 2 needles	0.001	165	10	5	0.16	567	0.06471±34	0.4942±78	0.05539±78	404.2	407.8	428.0
14 2 elongated prisms	0.003	358	23	5	0.17	2878	0.06778±34	0.5239±32	0.05605±20	422.8	427.7	454.5
15 3 small prisms	0.002	311	21	5	0.15	2090	0.07011±34	0.5380±36	0.05565±22	436.8	437.1	438.5
FB947 – MB rhyolite												
16 33 acicular prisms	0.027	446	23	13	0.48	22458	0.04981±24	0.3626±20	0.05281±8	313.3	314.2	320.6
17 7 fragments	0.030	266	15	9	0.31	14126	0.05513±26	0.4131±22	0.05435±8	345.9	351.1	385.5
18 11 needles	0.005	607	31	12	0.45	5475	0.04881±22	0.3532±20	0.05249±12	307.2	307.2	306.8
19 16 needles	0.010	508	26	13	0.48	3682	0.04870±22	0.3527±20	0.05252±12	306.6	306.7	308.0
BR1466 – AR rhyolite												
20 2 elongated prisms	0.001	403	25	6	0.21	1473	0.06482±36	0.4963±42	0.05553±32	404.9	409.2	433.6
21 single hollow prism	0.001	876	34	13	0.47	1044	0.03685±18	0.2672±28	0.05259±44	233.3	240.5	311.2
22 2 short prisms	0.001	88	4	13	0.47	182	0.04586±28	0.3318±152	0.05247±228	289.1	290.9	305.9
23 2 hollow prisms	0.001	374	16	5	0.15	794	0.04644±28	0.3368±60	0.05259±84	292.6	294.7	311.3
24 4 hollow prisms	0.003	374	19	12	0.44	1788	0.04850±24	0.3537±26	0.05289±26	305.3	307.5	324.0
25 4 prisms	0.002	546	30	8	0.26	2999	0.05551±26	0.4168±26	0.05445±18	348.2	353.7	389.9
26 5 small prisms	0.003	233	14	8	0.29	2314	0.05921±28	0.4465±34	0.05469±28	370.8	374.8	399.5

*: radiogenic; a: in mole-% relative to total radiogenic Pb; b: calculated on the basis of $^{208}\text{Pb}/^{206}\text{Pb}$ ratios, assuming concordancy; c: corrected for spike Pb and for fractionation; d: corrected for fractionation, spike, U and Pb blanks; no initial common Pb was present; error estimates (95% confidence level) refer to the last significant digits of the isotopic ratios and reflect reproducibility of standards, measurement errors and uncertainties in the common Pb correction.

(NESBITT and YOUNG, 1989). Samples that present such chemical modifications (Fig. 7, e.g. tuff and volcanoclastic layers) were classified according to relative proportions of reputedly immobile trace elements, as proposed in Nb/Y–Zr/TiO₂ classification diagram (Fig. 8; WINCHESTER and FLOYD;

1977). It must be kept in mind that this classification scheme yields only indicative information.

All samples that escaped intense chemical weathering (e.g. basal subaerial flows) were chemically classified according to the TAS diagram (Fig. 9; LE MAITRE, 1989), into which they

plot in good agreement to their respective mineralogy.

BASAL SUBAERIAL VOLCANISM

Chemical data for the subaerial lava flows outcropping along the western base of the Salvan-

DorénaZ trough are partly new (sample CN125, Tabs 2 and 3) and partly from PILLOUD (1991). They plot into the dacite and trachydacite fields of the TAS diagram (Fig. 9). These rocks have 63.5 to 66.2% SiO₂, are slightly peraluminous (A/CNK = 1.0–1.17), and alkali rich (Figs 9 and 10). They have chemical characteristics very similar to those

Tab. 2 Major and trace elements chemical composition for the analysed samples. See text for description and Annex 1 for location of samples. BSF = basal subaerial flow; MB = Mont-Blanc; ARR = Aiguilles-Rouges rhyolites.

Major elements (wt. %)	tuff layers										volcaniclastic layers				MB Rhyolites		ARR
	rhyolitic pebbles					*Fe ₂ O ₃ as total Fe					CN108	CN113	CN140	FB 947	MR2809	BR1466	
	CN125	CN252b	CN252d	CN118	CN121	CN122	CN256	CN256a	CN257	CN257a	CN108	CN113	CN140	FB 947	MR2809	BR1466	
SiO ₂	66.19	83.03	66.22	76.00	66.50	71.72	77.56	77.83	68.09	67.57	69.80	74.90	74.81	73.68	73.12	72.89	
TiO ₂	0.66	0.13	0.25	0.20	0.37	0.23	0.11	0.10	0.28	0.27	0.47	0.30	0.12	0.17	0.16	0.13	
Al ₂ O ₃	14.69	9.94	19.23	12.78	18.82	16.79	13.35	13.23	18.39	18.36	15.62	14.28	13.43	13.83	13.51	14.43	
*Fe ₂ O ₃	3.98	0.94	1.65	3.12	2.95	2.88	2.01	2.01	2.56	2.57	5.05	3.32	1.94	1.25	2.49	1.07	
MnO	0.05	0.01	0.01	0.04	0.08	0.02	0.02	0.02	0.04	0.04	0.07	0.02	0.03	0.05	0.11	0.02	
MgO	1.11	0.55	0.84	1.23	0.99	0.92	0.67	0.73	1.22	1.29	1.33	0.91	1.32	0.36	0.39	0.17	
CaO	2.34	0.03	0.08	0.31	0.52	0.08	0.04	0.06	0.14	0.17	0.58	0.04	0.81	1.03	1.06	0.56	
Na ₂ O	3.35	0.27	4.48	0.01	0.16	0.20	0.05	0.11	0.15	0.24	1.70	0.54	0.50	4.17	3.66	3.45	
K ₂ O	4.03	4.03	4.42	3.52	5.27	4.53	3.76	3.70	6.01	5.93	2.60	3.09	3.93	3.94	4.85	5.16	
P ₂ O ₅	0.25	0.03	0.05	0.09	0.08	0.04	0.02	0.02	0.09	0.09	0.06	0.03	0.04	0.06	0.15	0.41	
LOI	3.16	1.17	1.97	2.60	3.36	2.67	2.25	2.02	3.08	2.80	2.88	2.59	3.03	0.65	0.58	1.26	
Total	99.81	100.13	99.19	99.89	99.08	100.09	99.85	99.82	100.30	99.32	100.16	100.01	99.96	99.19	100.08	99.46	
Trace elements (ppm)																	
Nb	13	19	23	17	7	20	16	37	28	21	13	11	8	15	11	17	
Zr	204	103	173	156	254	239	170	162	165	148	392	120	124	140	113	64	
Y	30	17	6	46	57	57	38	26	33	3	42	48	43	28	20	9	
Sr	131	31	171	24	24	21	53	42	42	52	74	40	40	159	174	47	
Rb	166	173	217	213	314	263	289	196	202	266	175	176	171	152	142	404	
Ga	20	15	21	18	19	21	23	17	17	23	18	17	18	14	8	21	
Zn	60	41	26	61	40	46	29	46	39	31	82	56	84	42	82	42	
Co	33	41	23	22	14	25	7	2	6	5	29	25	16	28	45	-	
Cr	34	8	3	5	3	14	18	20	20	16	37	14	5	6	36	106	
V	60	13	23	13	25	25	21	11	14	22	44	46	5	12	12	5	
Ce	63	87	400	41	64	84	49	17	5	51	40	48	59	44	65	16	
Nd	30	35	151	20	40	45	25	11	<4<	29	19	24	31	14	24	14	
Ba	982	1485	1903	1194	914	753	941	529	508	755	392	496	2146	877	869	307	
La	38	46	286	22	47	54	27	10	5	26	25	18	49	14	32	33	
S	37	14	958	14	36	23	<3<	<3<	<3<	<3<	9	110	66	<10	-	-	
Sc	11	3	<2<	3	4	6	<2<	6	5	8	6	10	6	-	4	-	

Tab. 3 REE chemical composition for the analyzed samples. See text for description and Annex 1 for location of samples.

REE	Samples								
	CN125	CN118	CN121	CN122	CN113	CN140	MR2809	FB803	BR1466
La	28.8	35.1	21.2	34.4	36.5	28.6	32.0	39.8	33.2
Ce	64.2	77.9	51.0	77.2	77.3	64.0	65.4	73.3	16.0
Pr	7.6	8.9	5.6	8.9	9.3	6.9	7.2	6.8	-
Nd	28.0	32.3	20.3	30.5	33.8	24.6	24.5	24.7	13.8
Sm	5.8	6.7	4.1	6.0	6.8	5.2	4.9	5.6	3.13
Eu	1.01	0.50	0.81	0.61	0.78	0.54	0.95	0.77	0.31
Gd	5.7	6.1	4.0	5.4	5.4	5.1	5.0	5.8	2.53
Tb	0.82	0.95	0.80	0.90	0.84	0.74	0.80	0.94	-
Dy	4.8	5.4	5.7	5.7	4.8	4.5	4.2	5.6	2.0
Ho	0.94	1.09	1.29	1.22	0.98	0.94	0.84	1.20	-
Er	2.4	3.1	3.7	3.5	2.8	2.6	2.6	3.4	0.94
Yb	2.1	2.8	3.1	3.3	2.8	2.7	2.7	3.4	0.81
Lu	0.30	0.42	0.49	0.51	0.44	0.41	0.45	0.53	0.41
Hf	2.9	4.3	6.1	7.2	3.1	3.4	-	5.6	-
Ta	1.8	1.8	1.3	2.6	2.6	1.6	-	1.6	-
Pb	17.8	6.4	9.2	29.1	169.4	29.2	-	17.2	-
Th	10.8	13.3	13.0	18.3	17.7	12.0	18.5	22.0	-
U	4.5	5.6	6.0	5.5	7.2	3.7	8.8	5.5	-

of the dacitic dykes from the Aiguilles-Rouges basement (BRÄNDLEIN, 1991; BRÄNDLEIN et al., 1994) both in terms of major and trace element concentrations – in particular high Ba contents (760–980 ppm) – but differentiate from them for their higher contents in K₂O and Na₂O. A feature common to all the samples is their high K content (Fig. 10), as frequently observed for melts occurring in thickened continental crusts.

The initial ϵ Nd of sample CN125 (Tab. 4), recalculated at 308 Ma, is the most negative (–7.14) of the analyzed volcanic samples, close to typical values for crustal-derived peraluminous granites (e.g. VOSHAGE et al., 1990).

Tab. 4 Whole-rock Nd isotopic data for the volcanic rocks of the Salvan-Dorénaz basin. Data have been normalized to $^{146}\text{Nd}/^{144}\text{Nd} = 0.7219$ (WASSERBURG et al., 1981). Uncertainties refer to the last significant digits of the isotopic ratios. Time for ϵ Nd(t) calculations for undated samples has been arbitrarily set to 300 Ma.

Samples	$^{143}\text{Nd}/^{144}\text{Nd}$	τ (Ma)	$\epsilon\text{Nd}_{(t)}$
CN125	0.512100 ± 74	308	–7.14
CN113	0.512530 ± 28	300	0.77
CN121	0.512544 ± 30	300	1.02
CN122	0.512433 ± 20	300	–1.02
CN140	0.512180 ± 19	300	–6.3
CN118	0.512267 ± 20	295	–4.56

VOLCANIC PEBBLES

Two volcanic pebbles were analyzed (Tabs 2 and 3), and they show abnormal major element compositions (e.g. very low Ca contents) indicating intense weathering (Fig. 7). Sample CN252b is very high in Si (83% SiO₂) and depleted in Na, pointing to silicification processes either early within the ignimbritic flows or subsequently within the sedimentary basin. It plots into the trachy-andesite field of the Nb/Y–Zr/TiO₂ diagram (Fig. 8). Its low Sr (31 ppm) and very high Ba (1485 ppm) contents also might reflect fluid circulation effects. Conversely, sample CN252d has only 66% SiO₂ and plot into the trachyte field (Fig. 8). Its very high contents in Al₂O₃ (19.23%), Ba (1900 ppm) and REE (e.g. 286 ppm of La) suggest the occurrence of xenolithic material, such as a micaeous restitic clots.

TUFF LAYERS

Seven samples of tuff layers from the Salvan-Dorénaz sedimentary basin have been analyzed (Tabs 2 and 3). They have a wide range of compositions (SiO₂ = 67.6–77.8%) and plot into the trachyte and trachy-andesitic (close to the rhyolites) fields (Fig. 8). As briefly mentioned above, they all

present very low Ca and Na values and often are high in K and Al, reflecting alteration of the feldspathic component into illitic material (Fig. 7; NESBITT and YOUNG, 1989). Sr behaves as Ca (Fig. 12), whereas concentrations in other mobile trace elements such as Ba and Rb are very variable (e.g. samples CN256 and 256a, Tab. 2). REE concentrations are higher than in the rhyolitic dykes from the Aiguilles-Rouges basement, but very similar to those of the basal dacitic flows and of the Mont-Blanc granite and rhyolites (Tab. 3 and Fig. 11).

Initial ϵNd are very heterogeneous (Tab. 4), ranging from negative values (-4.56 , CN118) typical for Late-Variscan granitic rocks of the area (BUSSY, unpub. data) to slightly positive values (1.02 , CN121), unknown in this region and characteristic of mantle-derived material. This high range of values can be explained by wall rock assimilation processes and/or by admixture of detrital (crustal) material to initial melts, to which contributed mantle reservoirs. Additional data are necessary to confirm this first set of results.

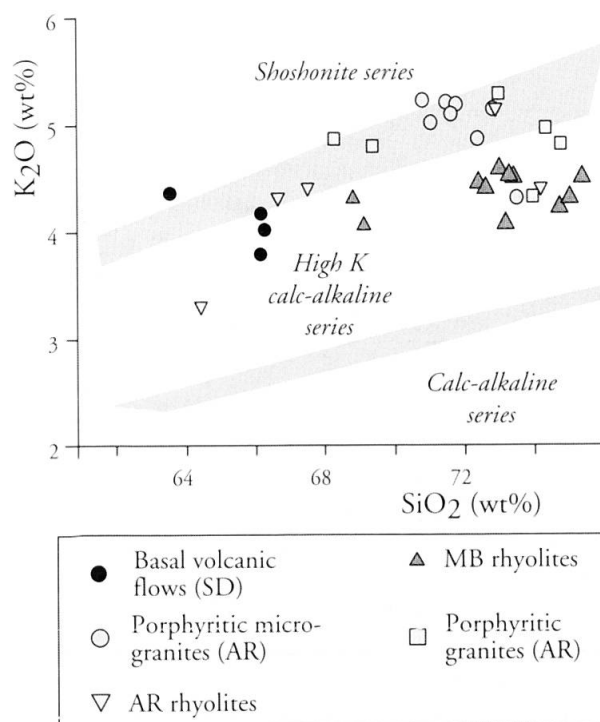


Fig. 10 K_2O vs SiO_2 diagram for subdivision of subalkaline rocks. All the considered volcanic samples from the Aiguilles-Rouges and Mont-Blanc massifs show a high-K calc-alkaline affinity. Shaded bands are boundary lines after different authors (ROLLINSON, 1993). New data are reported in table 2. Data compared from the literature are those of: PILLOUD (1991) for the basal dacitic flows; BRÄNDLEIN (1991), BRÄNDLEIN et al. (1994) and LERESCHE (1992) for the Aiguilles-Rouges subvolcanic dykes; MARRO (1986) and BURRI and MARRO (1993) for the Mont-Blanc rhyolites.

VOLCANICLASTIC DEPOSITS

Three volcanoclastic sandstone layers from the upper part of the Salvan-Doréna basin have been analyzed (CN108, 113, 140, Tab. 2). Their silica content ranges from 69.8 to 74.9% SiO_2 and they plot into the dacite-rhyodacite fields (Fig. 8). Although non-volcanic detrital material has been identified in these lithologies, their overall chemical composition is not very different from that of other investigated volcanic rocks. They present erratic contents in mobile trace elements (e.g. Ba, Tab. 3). Again, the highly variable initial ϵNd values (e.g. 0.77 and -6.03 , Tab. 4) of these volcanoclastic layers, as illustrated by the otherwise very similar samples CN113 and CN140 (Tab. 2), probably reflect mixing processes between crustal and mantle-derived materials.

AIGUILLES-ROUGES SUBVOLCANIC DYKES

Chemical data for the Aiguilles-Rouges subvolcanic rocks are reported in BRÄNDLEIN (1991), LERESCHE (1992) and BRÄNDLEIN et al. (1994). A first group of volcanic dykes outcrops in the Salanfe (red rhyolites, e.g. sample BR1466) and Collonges areas and is characterized by 70.8 to 73.5% of SiO_2 and $> 5\%$ of K_2O . They plot into the rhyolite field of the TAS diagram (Fig. 9). A second group of dykes is distinctly less acidic with 62.8 to 67.5% of SiO_2 and 3–4.4% of K_2O and they are classified as dacites (Fig. 9; gray rhyolites, Col des Montets area). All rocks are strongly peraluminous ($A/\text{CNK} > 1.4$).

The rhyolites have a chemical composition typical of evolved acidic rocks, with rather low Ca and Sr contents (0.55–1.1% and 34–116 ppm, respectively), high Rb contents (250–400 ppm) (Fig. 12) and marked negative Eu anomalies (Fig. 11). They are very similar to the evolved facies of the Vallorcine granite (BRÄNDLEIN et al., 1994) and probably derive from the latter. The dacites have trace element characteristics of rocks less evolved than the mafic facies of the Vallorcine granite (BRÄNDLEIN et al., 1994; e.g. $> 2.3\%$ CaO, > 220 ppm Sr, < 230 ppm Rb, 450–1000 ppm Ba).

MONT-BLANC RHYOLITES

Chemical data for the Mont-Blanc rhyolites are those of MARRO (1986) and BUSSY (1991). Their silica content ranges between 69 and 75% SiO_2 and they all plot in the rhyolite field of the TAS diagram (Fig. 9). These rocks are slightly peraluminous (A/CNK around 1.05) and high in total

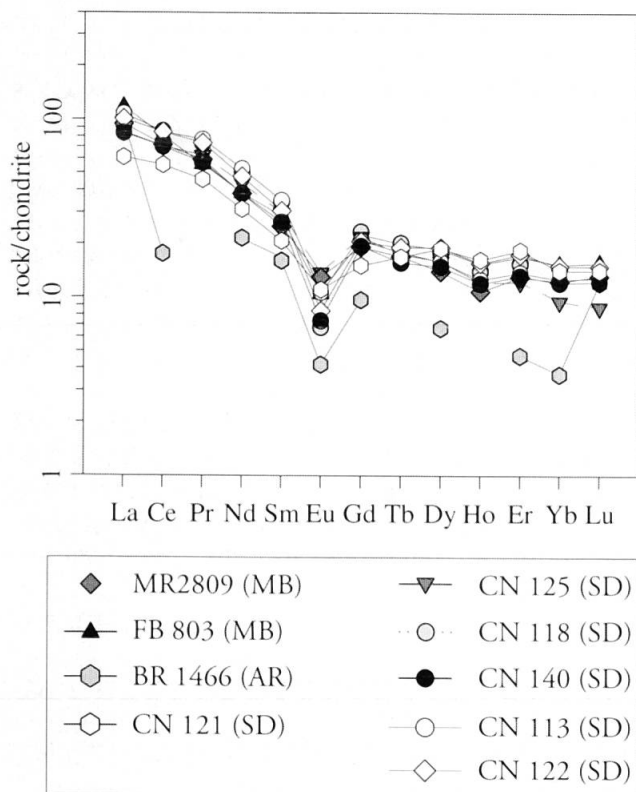


Fig. 11 Rare Earth Elements patterns for the Salvan-Dorénaz (SD) volcanic and volcanigenic deposits and for Aiguilles-Rouges (AR) and Mont-Blanc (MB) sub-volcanic dykes. Data reported in table 3. Normalizing values for chondrites after WAKITA *et al.* (1971).

alkalis (Fig. 9). Their overall major element (Tab. 2) and REE (Tab. 3 and Fig. 11) composition is in keeping with the chemical evolutionary trend of the neighboring Mont-Blanc granitic rocks (MARRO, 1987), except for slightly lower K_2O contents (3.9–4.5%) relative to their differentiation index. On the other hand, there are differences for some trace elements (Fig. 12), such as Sr (higher in the rhyolites, 130–250 ppm), Rb (lower at 160–190 ppm) and Ba, which is much higher in the rhyolites (760–1060 ppm) than in the granites (480–600 ppm). Post-emplacment hydrothermal fluid circulation along the rhyolitic dykes might be partly responsible for the contrasting concentrations in mobile elements, although the higher Ba values might indicate different magma sources.

Discussion

According to the geochronological time scale for the Late Palaeozoic of continental Western Europe (MENNING, 1995), age determinations on volcanic and volcanigenic layers from the Salvan-Dorénaz basin indicate only Late Carboniferous ages for the synsedimentary volcanic activity. In

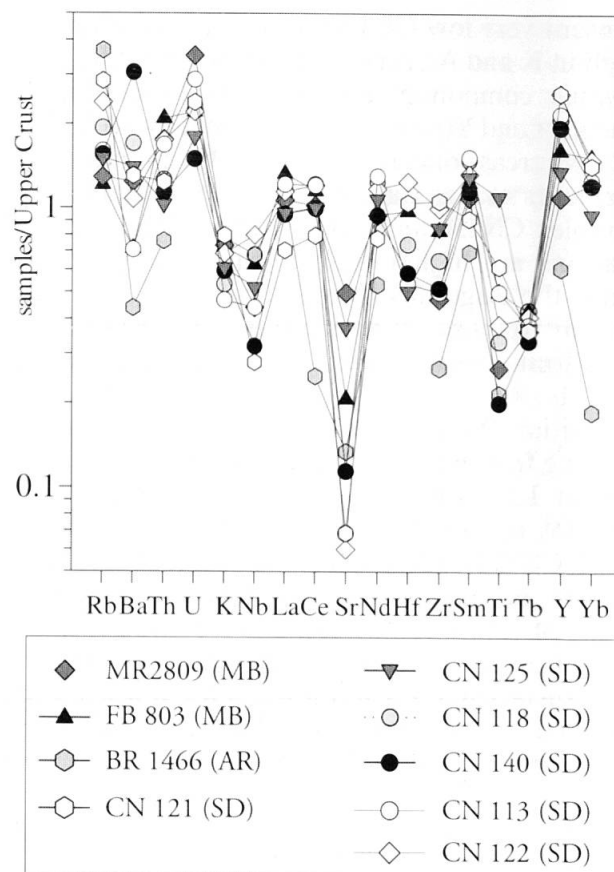


Fig. 12 Trace elements concentration for the Salvan-Dorénaz (SD) volcanic and volcanigenic deposits and for Aiguilles-Rouges (AR) and Mont-Blanc (MB) sub-volcanic dykes. Data reported in tables 2 and 3. Normalizing values for Upper Crust after (TAYLOR and MC LENNAN, 1981). See text for discussion.

this continental basin the lower limit for elastic deposition is set by dacitic subaerial flows outcropping along its northwestern base (Fig. 3) and emplaced at around 308 ± 3 Ma (Fig. 6). The youngest sediments outcropping in its northern areas are about 295 Ma old, as determined on a tuff layer (Fig. 6) located ~200 m below the angular unconformity with the shallow marine Triassic deposits (Fig. 3). Therefore, no volumetrically important Permian sediments are currently preserved within the Salvan-Dorénaz basin.

The dacitic flows outcropping at the base of the Salvan-Dorénaz erupted along the western faulted margin of the subsiding trough, possibly as lava domes, as commonly observed in other Late Palaeozoic sedimentary basins (e.g. Seui basin, Sardinia, CORTESOGNO *et al.*, 1998; Collio basin, Southern Alps, BREITKREUZ *et al.*, 1999). The western border fault of the Salvan-Dorénaz trough is considered a major tectonic structure presenting similar orientation to the neighboring Vallorcine granite and to several subvolcanic

dykes. Furthermore, the Vallorcine granite and the nearby Aiguilles-Rouges subvolcanic dykes are considered cogenetic on the base of their field relations, geochemistry (BRÄNDLEIN et al., 1994) and zircon typology (Fig. 5). Considering the age and geochemical characters of the dacitic flows, we interpret them as the surface equivalent of the subvolcanic dacitic dykes outcropping in the surrounding Aiguilles-Rouges basement. As the strongly negative initial ϵNd value (-7.14) indicates, these peraluminous dacitic melts most likely derive from crustal sources, as the coeval Vallorcine granitic magmas (BRÄNDLEIN et al., 1994), but they could represent distinct batches generated at slightly higher partial fusion rates. Melts were possibly collected directly from the magma production zones, which would account for the low differentiation index of the erupted material.

The ignimbritic pebbles from the lower levels of the Salvan-Dorénaz sedimentary record have no equivalent lithologies in the surrounding basement. They represent the only evidence of ignimbritic volcanism in the Aiguilles-Rouges massif. Although undated, their undeformed textures suggest Late Carboniferous eruption ages.

Considering the tuffs and volcanoclastic layers sampled in the upper levels of the Salvan-Dorénaz basin, their ages, zircon typology and some of their ϵNd values are in sharp contrast with all the previously discussed volcanic rocks. These features together with their very fine textures point to distant eruptive centers and to contrasted magma sources. The few positive ϵNd values measured (< 1.02) might confirm a prominent mantellic source, although coexisting negative values as low as -6 cast doubt on the reliability of the data as genetic tracers. Additional data are needed to evaluate if these contrasting values are original (i.e. evidencing blending of crustal and mantellic materials) or linked to subsequent sedimentary processes (e.g. mixing with crustal sediments, alteration). High A index zircons are typically found in late- to post-orogenic alkaline granitoids (e.g. the 303 Ma Mont-Blanc granite, BUSSY, 1990). Despite similar zircon typologies (Fig. 5), the Mont-Blanc magmatism (granite and rhyolites) is too old to be the source of these tuff layers. Alkali-calcic to alkaline magmas with similar zircon typology and REE concentrations are known from adjacent areas, like in the Aar and Gotthard External Crystalline massifs (SCHALTEGGER and CORFU, 1992; BONIN et al., 1998). There, plutonic and volcanic rocks (breccia, ignimbrites and lapilli tuffs) have been dated between 300 and 298 ± 2 Ma (SCHALTEGGER and CORFU, 1992; 1995). Similar tuff layers occurring

in a different Permocarboneous trough in northern Switzerland (Weiach drill site) located 100 km north of the Aar massif have been already linked to this magmatic activity (SCHALTEGGER, 1997a). The Salvan-Dorénaz tuffs could as well derive from the same magmatic center, or alternatively from similar ones located in the same distance range around the Aiguilles-Rouges massif.

Within the Mont-Blanc massif, the rhyolitic dykes and the adjacent granite intrusion have an indisputable genetic link, as pointed out by whole-rock chemistry and zircon typology. Deep crustal and mantellic magma sources are inferred (BUSSY, 1990). On the other hand, the time relationships between intrusive and subvolcanic magmatism are much less clear. According to BURRI and MARRO (1993), there is a primary igneous contact between rhyolitic dykes and the marginal facies of the Mont-Blanc granite. As rock textures suggest shallower injection levels for the rhyolites than for the coarse-grained granite, a younger intrusion age was inferred for the rhyolites in a context of tectonic exhumation. On the other hand, the dated rhyolite sample (307 ± 2 Ma, Fig. 6, FB947) is older than, or just contemporaneous to the 303 ± 2 Ma Mont-Blanc granite within uncertainties. Considering the perfectly euhedral shape of the rhyolite zircons and the large number of grains analyzed, it is unlikely that we dated an inherited zircon population, but rather the time of zircon growth within the rhyolitic melt, which should not be significantly different from the intrusion age. If true, the rhyolite dyke swarm must have been brought into contact with the granite through tectonic movements at time of granite intrusion or subsequently.

All dated samples contain inherited zircon populations about 350, 450 or 600 Ma old, incorporated into the volcanic material either in the production zone of the magmas, or during their ascent and/or their final emplacement. A sedimentary input is also possible for the tuff and volcanoclastic layers. Ages of 600 and 450 Ma are well represented in the External Crystalline massifs. Gondwana-derived Pan-African zircons (ca. 600 Ma) are commonly found as inherited grains in Variscan granites and paragneisses, whereas 440–460 Ma old orthogneisses are present in all basement units of the Alps (e.g. BUSSY and VON RAUMER, 1993; SCHALTEGGER and CORFU, 1992; SCHALTEGGER, 1994; GEBAUER, 1993; BERTRAND et al., 2000). The 350 Ma old zircons are more puzzling, as no magmatic rock of that age has been presently identified in the Aiguilles-Rouges and Mont-Blanc areas. Possibly, they might derive from tonalitic melts formed during decompression and uplift of the eclogitic units at the south-

ern end of the Aiguilles-Rouges massif (VON RAUMER *et al.*, 1996).

The volcanoclastic sandstone (sample CN140) highlights the difficulty of interpreting zircon ages in acidic volcanic deposits. These quenched magmas do not have time to crystallize significant amounts of zircons, whereas they host many inherited grains, which are not always resorbed. As a consequence, euhedral crystals from an inherited population can easily be selected for U–Pb analysis and produce a coherent set of data that can be erroneously interpreted as the magmatic age of the rock. In the absence of other stratigraphical indicators and/or of fossils in adjacent sedimentary rocks, this Late Carboniferous layer would have been interpreted as a Silurian deposit. This problem must be kept in mind when dating volcanic rocks in metamorphic environments.

Geotectonic implications

The post-collisional evolution of the thickened Variscan crust in the Aiguilles-Rouges area is characterized by fast exhumation in a transcurrent tectonic regime along subvertical N–S to NNE–SSW fault zones. Decompression melting occurred at 320 Ma (BUSSY *et al.*, 2000) at a pressure of about 4 kbar (ca. 12 km) in a ductile dextral shear regime (SCHULZ and VON RAUMER, 1993). At 307 Ma, these lithologies were syntectonically intruded along similar NNE–SSW fracture zones by the Vallorcine granite. The fine-grained fabric of its upper facies and the devitrified subvolcanic textures of its associated dykes point to shallow-level intrusion, possibly less than 2–3 km, which therefore would set the exhumation rate for basement units at an order of magnitude of 1 mm/a. Subsequent deformation occurred when the rocks were increasingly colder, to end up with subvertical low-T mylonitic foliation and C-S structures.

At about the time of the Vallorcine granite emplacement (308 Ma) started the tectonic subsidence of the Salvan-Dorénaz trough, sliding along a major fault with a similar direction to that along which intruded the Vallorcine granite. High-grade metamorphic rocks and Late Variscan granitoids were eroded from adjacent heights and accumulated as clastic sediments within the basin (CAPUZZO, unpub. data). The coherent time frame achieved for the basin formation and filling through isotopic age determination is a pre-requisite for modeling sedimentation and subsidence rates within the basin. A short time span of 10–15 Ma is suggested for the sedimentary evolution of the Salvan-Dorénaz basin, thus inferring a con-

servative estimation of long term, average subsidence rates in the order of magnitude of 0.1 mm/a. This value has to be considered as the very minimum, since it was determined from the maximum time span of 15 Ma for the basin evolution and from a conservative estimation of 1500 m thick for its sedimentary record. Nevertheless, it is in agreement with other available data for Permian–Carboniferous basins in the Alps (e.g. SCHALTEGGER and BRACK, 1999), and denote high average subsidence rates typical in tectonically controlled continental basins (NILSEN and SYLVESTER, 1995).

The sedimentary record in the Salvan-Dorénaz basin stops at 295 +3/–4 Ma. Younger deposits either never existed or were eroded during a phase of tectonic inversion, possibly induced by Permian transpressive movements along the marginal faults of the trough, as also suggested by the regional erosional unconformity that separate the Late Carboniferous sediments from the overlying Triassic shallow marine deposits.

The undeformed red rhyolite dykes of the Aiguilles-Rouges massif (BR1466) sets the final age for ductile deformation in this massif at 294 Ma (more probably around 300 Ma). Unfortunately the accuracy of this data does not allow any further precision.

Conclusions

The Late Variscan tectono-magmatic evolution in the Aiguilles-Rouges and Mont-Blanc massifs is governed by post-collisional processes that restored the thickened continental lithosphere to normal size. Basement units experienced fast tectonic exhumations (ca. 1 mm/a) in a transtensional tectonic regime, while localized areas underwent rapid tectonic subsidence and were filled with thick continental sediments. In these two massifs intense magmatic activity occurred around 307 Ma at different crustal to subvolcanic levels, while coeval subaerial volcanism is today preserved only along the western base of the Salvan-Dorénaz basin. Intrusion and extrusion of melts was strongly controlled by wrench tectonism occurring along major N–S to NNE–SSW fracture zones. Geochemistry and zircon typology of melts indicate contrasting origin: a common anatectic peraluminous source for the Salvan-Dorénaz basal volcanism, the Vallorcine granite and the Aiguilles-Rouges subvolcanic dykes; a mixing of mantle melts with crustal sources for the Mont-Blanc granite and for the Mont-Blanc rhyolites.

Subsequent volcanic activity, occurring at 295 +3/–4 Ma, is documented by tuff layers occurring

only within the Salvan-Dorénaz continental basin. Field features suggest origin from highly explosive and distant volcanic centers, and zircon typology is in keeping with the general tendency of the Late Variscan volcanism to evolve toward increased alkalinity with stronger mantellic contribution. They might come from coeval, explosive volcanism located in the Aar-Gotthard massif.

In the Salvan-Dorénaz basin, age determinations of synsedimentary volcanic deposits indicate only Late Carboniferous volcanic activity (308–295 Ma), therefore no significant Permian deposits are preserved within its stratigraphic record. The calculated long term, minimum subsidence rates during basin evolution are in the order of magnitude of > 0.1 mm/a.

Acknowledgements

We acknowledge the financial support by the Swiss National Science Foundation (NC: grants No. 21–43103.95 and 20–50484.97 to A. Wetzel), (FB: grant No. 21–45650.95 to J. Hernandez). We are sincerely thankful to J. von Raumer and an anonymous reviewer who helped us with their comments to significantly improve the paper, and to A. Wetzel for his suggestions on an early version of the manuscript. We benefited from many discussions with J. von Raumer and we thank him for supplying us with samples and data from his personal collection. We warmly thank J. Lavanchy, H.R. Pfeifer, J. Hunziker (Lausanne) for their help and support during geochemical and mineral separation analyses; W. Stern (Basel) for the XRD analyses; H. Lapiere (Grenoble) for the REE data and isotopic separations; I. Kramers (Bern) for the Nd isotopic measurements; D. Davis (Toronto) for the facilities to the geochronological laboratory of the Royal Ontario Museum.

References

ARTHAUD, F. and MATTE, P.H. (1977): Late Palaeozoic strike-slip faulting in Southern Europe and Northern Africa. *Geol. Soc. Am. Bull.* 88, 1305–1320.
 BANZET, G., LAPIERRE, H., LE FORT, P. and PECHER, A. (1985): Le volcanisme Carbonifère-Supérieur du Massif des Grandes Rousses (zone Dauphinoise-Alpes Externes Françaises): un magmatisme à affinités shoshonitiques lié à la fracturation crustale tardivarisque. *Géol. Alpine* 61, 33–60.
 BARRAT, J.A., KELLER, F., AMOSSE, J., TALOR, R.N., NESBITT, R.W. and HIRATA, T. (1996): Determination of rare earth elements in sixteen silicate reference samples by ICP-MS after Tm addition and ion exchange separation. *Geostd. Newslett.* 20, 133–139.
 BECO-GIRAUDON, J.F. (1993): Problèmes de la biostratigraphie dans le Paléozoïque Supérieur continental (Stéphanien-Autunien) du Massif Central. *Geodin. Acta* 6, 219–224.
 BENEK, R., KRAMER, W., MCCANN, T., SCHECK, M., NEGENDANK, J.F.W., KORICH, D., HEUBSCHER, H.-D. and BAYER, U. (1996): Permo-Carboniferous magmatism of the Northeast German Basin. *Tectonophysics* 266, 379–404.

BERTRAND, J.M., PIDGEON, R.T., LETERRIER, J., GUILLOT, F., GASQUET, D. and GATTIGLIO, M. (2000): Shrimp and conventional U–Pb geochronology of Pre-Alpine basement rocks from the Briançonnais and Piemontese domains of Western Alps (Savoie, Valle d’Aosta and Piemont). *Tectonophysics*, in press.
 BONIN, B., BRÄNDLEIN, P., BUSSY, F., DESMONS, J., EGGENBERGER, U., FINGER, F., GRAF, K., MARRO, CH., MERCOLLI, I., OBERHÄNSLI, R., PLOQUIN, A., VON QUADT, A., VON RAUMER, J., SCHALTEGGER, U., STEYRER, H., VISONÀ, D. and VIVIER, G. (1993): Late Variscan magmatic evolution of the Alpine basement. In: VON RAUMER, J.F. and NEUBAUER, F. (eds): *Pre-Mesozoic Geology in the Alps*. Springer-Verlag, 171–201.
 BONIN, B., AZZOUNI-SEKKAL, A., BUSSY, F. and FERRAG, S. (1998): Alkali-calcic to alkaline post-collision granite magmatism: petrologic constraints and geodynamic settings. *Lithos* 45, 45–70.
 BOVAY, P. (1988): *Pétrographie et géochimie d’une association de roches acides et basiques, Massif cristallin de Fully (Valais)*. Unpubl. Diploma Thesis, Univ. Lausanne, Switzerland, 59 pp.
 BRÄNDLEIN, P. (1991): *Petrographische und geochemische Charakteristika des Vallorcine-Granits, Aiguilles-Rouges-Massiv (Westalpen, Schweiz)*. Unpubl. Ph.D. Thesis, Univ. Freiburg, Switzerland, 99 pp.
 BRÄNDLEIN, P., NOLLAU, G., SHARP, Z. and VON RAUMER, J. (1994): Petrography and geochemistry of the Vallorcine granite (Aiguilles-Rouges massif, Western Alps). *Schweiz. Mineral. Petrogr. Mitt.* 74, 227–243.
 BREITKREUZ, C., CHECCHIA, C., CASSINIS, G., CORTESOGNO, L. and GAGGERO, L. (1999): Dynamic of a Variscan post-orogenic basin in the Southern Alps: sublacustrine SiO₂-rich volcanism and associated mass flows (Collio basin, Italy). *J. Conf. EUG 10 Abstr.* 4, 294–295.
 BROUTIN, J., DOUBINGER, J., LANGIAUX, X. and PRIMEY, D. (1986): Conséquences de la coexistence de flores à caractères stéphanien et autunien dans les bassins limniques d’Europe occidentale. *Mem. Soc. Géol. Gr.* 149, 15–25.
 BURG, J.-P., VAN DEN DRIESSCHE, J. and BRUN, J.-P. (1994): Syn- to post-thickening extension in the Variscan belt of Western Europe: modes and structural consequences. *Géologie de la France* 3, 33–51.
 BURRI, M. and MARRO, C. (1993): Atlas géologique de la Suisse 1:25.000, feuille 1345: Orsières (avec notice explicative). *Comm. Géol. Suisse*, 75 pp.
 BUSSY, F. (1990): Pétrogenèse des enclaves microgrenues associées aux granitoïdes calco-alkalins: exemple des massifs Varisque du Mont-Blanc (Alpes occidentales) et Miocène du Monte Capanne (Ile d’Elbe, Italie). *Mémoires de Géologie (Lausanne)* 7, 309 pp.
 BUSSY, F. and VON RAUMER, J.F. (1993): U–Pb dating of Palaeozoic event in the Mont-Blanc crystalline massif, Western Alps. *Terra Nova* 5 suppl. 1, 382–383.
 BUSSY, F. and CADOPPI, P. (1996): U–Pb zircon dating of granitoids from the Dora-Maira massif (western Italian Alps). *Schweiz. Mineral. Petrogr. Mitt.* 76, 217–233.
 BUSSY, F., DELITROZ, D., FELLAY, R. and HERNANDEZ, J. (1997): The Pormenaz monzonite (Aiguilles-Rouges, western Alps): an additional evidence for a 330 Ma-old magnesio-potassic magmatic suite in the Variscan Alps. *Schweiz. Mineral. Petrogr. Mitt.* 78, 193–194.
 BUSSY, F. and HERNANDEZ, J. (1997): Short-lived bimodal magmatism at 307 Ma in the Mont-Blanc/Aiguilles-Rouges area: A combination of decompression melting, basaltic underplating and crustal fracturing. 3rd workshop on Alpine Geological Studies,

- Oròpa-Biella. *Quaderni di Geodinamica Alpina e Quaternaria* 4, 22.
- BUSSY, F., HERNANDEZ, J. and VON RAUMER, J. (2000): Bimodal magmatism as a consequence of the post-collisional readjustment of the thickened Variscan continental lithosphere (Aiguilles-Rouges and Mont-Blanc massifs, Western Alps). *Trans. Royal Soc. Edinburgh*, in press.
- CAPUZZO, N., WETZEL, A. and NIKLAUS, P.A. (1997): Tectonic cyclothems document the history of a Late Palaeozoic fluvial basin (Dorénaz basin, southwestern Switzerland). *Terra Nova* 9 (suppl. 1), 99.
- CAPUZZO, N. and BUSSY, F. (2000): Syn-sedimentary volcanism in the Late Carboniferous Salvan-Dorénaz basin (Western Alps). *Mem. Sci. Nat. Brescia*, submitted.
- CASSINIS, G., TOUTIN-MORIN, N. and VIRGILI, C. (1992): A general outline of the Permian continental basins in Southwestern Europe. In: SWEET, W.C., YANG, Z.Y., DICKINS, J.M. and YIN, H.F. (eds): *Permo-Triassic events and their global correlation*. Cambridge University press, 41–50.
- CORTESOGNO, L., CASSINIS, G., DALLAGIOVANNA, G., GAGGERO, L., OGGIANO, G., RONCHI, A., SENO, S. and VANOSI, M. (1998): The Variscan post-collisional volcanism in Late Carboniferous–Permian sequences of Ligurian Alps, Southern Alps and Sardinia (Italy): a synthesis. *Lithos* 45, 305–328.
- DEBON, F. and LEMMET, M. (1999): Evolution of Mg/Fe ratios in late Variscan plutonic rocks from the External Crystalline Massifs of the Alps (France, Italy, Switzerland). *J. Petrol.* 40, 1151–1185.
- DOBMEIER, C. (1996): *Geodynamische Entwicklung des südwestlichen Aiguilles-Rouges-Massivs (Westalpen, Frankreich)*. *Mémoires de Géologie (Lausanne)* 29, 198 pp.
- DOBMEIER, C. (1998): Variscan P-T deformation paths from the southwestern Aiguilles Rouges massif (External massif, western Alps) and their implication for its tectonic evolution. *Geol. Rundsch.* 87, 107–123.
- DOBMEIER, C., PFEIFER, H.R. and VON RAUMER, J.F. (1999): The newly defined “Greenstone Unit” of the Aiguilles-Rouges massif (Western Alps): remnant of an early Palaeozoic oceanic island-arc? *Schweiz. Mineral. Petrogr. Mitt.* 79, 263–276.
- FRANKS, G.D. (1968): A study of Upper Palaeozoic sediments and volcanics in the northern part of the eastern Aar Massif. *Ecolgae geol. Helv.* 61, 49–140.
- FREY, M., DESMONS, J. and NEUBAUER, F. (1999): Metamorphic map of the Alps. *Schweiz. Mineral. Petrogr. Mitt.* 79.
- GEBAUER, D. (1993): The pre-Alpine evolution of the continental crust of the Central Alps – an overview. In: VON RAUMER, J.F. and NEUBAUER, F. (eds): *Pre-Mesozoic Geology in the Alps*. Springer Verlag, 93–117.
- HENK, A. (1999): Did the Variscides collapse or were they torn apart?: A quantitative evaluation of the driving forces for postconvergent extension in central Europe. *Tectonics* 18, 774–792.
- IRVINE, T.N. and BARAGAR, W.R. (1971): A guide to the chemical classification of the common volcanic rocks. *Can. J. Earth Sci.* 8, 523–548.
- JONGMANS, W.J. (1960): *Die Karbonflora der Schweiz*. *Beitr. geol. Karte Schweiz*, 108.
- KRAINER, K. (1993): Late and post-Variscan sediments of the Eastern and Southern Alps. In: VON RAUMER, J.F. and NEUBAUER, F. (eds): *Pre-Mesozoic Geology in the Alps*. Springer Verlag, 537–564.
- KROGH, T.E. (1973): A low-contamination method for hydrothermal decomposition of zircon and extraction of U and Pb for isotopic age determinations. *Geochim. Cosmochim. Acta* 37, 485–494.
- KROGH, T.E. (1982): Improved accuracy of U–Pb zircon ages by the creation of more concordant system using an air abrasion technique. *Geochim. Cosmochim. Acta* 46, 637–649.
- LE MAITRE, R.W. (1989): *A classification of igneous rocks and glossary of terms*. Blackwell Scientific Publications, Oxford, 193 pp.
- LERESCHE, S. (1992): *Pétrographie et géochimie des Microgranites des Monts de Collonges et des Roches Associées (Massif des Aiguilles-Rouges, Valais)*. Unpubl. Diploma Thesis, Univ. Lausanne, Switzerland, 84 pp.
- LUDWIG, K. (1999): *Isoplot/Ex. A Geochronological Toolkit for Microsoft Excel*. Geochronology Center spec. publ. 1a.
- MARRO, C. (1986): *Les Granitoides du Mont Blanc en Suisse*. Unpubl. Ph.D. Thesis, Univ. Fribourg, Switzerland, 145 pp.
- MARRO, C. (1987): *Histoire des granitoides du Mont Blanc en Suisse*. *Bull. Soc. Frib. Sc. Nat.* 76, 73–128.
- MATTE, P. (1991): *Accretionary history and crustal evolution of the Variscan belt in Western Europe*. *Tectonophysics* 196, 309–337.
- MATTER, A. (1987): *Faciesanalyse und Ablagerungsmilieus des Permokarbons im Nordschweizer Trog*. *Ecolgae geol. Helv.* 80, 345–367.
- MENNING, M. (1995): A numerical time scale for the Permian and Triassic periods: an integrated time analysis. In: SCHOLLE, P.A., PERYT, T.M. and ULMER-SCHOLLE, D.S. (eds): *The Permian of Northern Pangaea*. Springer Verlag, 77–97.
- MORARD, A. (1998): *Pétrographie et cartographie du socle du massif du Mont-Blanc dans la région de la Montagne de Lognan (Argentière, France)*. Unpubl. Diploma Thesis, Univ. Lausanne, Switzerland, 178 pp.
- NESBITT, H.W. and YOUNG, G.M. (1984): Prediction of some weathering trends of plutonic and volcanic rocks based upon thermodynamic and kinetic considerations. *Geochim. Cosmochim. Acta* 48, 1523–1534.
- NESBITT, H.G. and YOUNG, G.M. (1989): Formation and diagenesis of weathering profiles. *J. Geol.* 97, 129–147.
- NIKLAUS, P.-A. and WETZEL, A. (1996): *Faziesanalyse und Ablagerungsmilieu der fluviatilen Sedimentfüllung des Karbontroges von Salvan-Dorénaz*. *Ecolgae geol. Helv.* 89, 427–437.
- NILSEN, T.H. and SYLVESTER, A.G. (1995): Strike-slip basins. In: BUSBY, C.J. and INGERSOLL, R.V. (eds): *Tectonics of sedimentary basins*. Blackwell Science, Oxford, 425–457.
- OULIANOFF, N. (1924): *Le massif de l'Arpille et ses abords*. *Mat. Carte géol. Suisse* 54 (2 part.), 66 pp.
- PILLOUD, C. (1991): *Structures de déformation alpines dans le synclinal de Permo-Carbonifère de Salvan-Dorénaz (massif des Aiguilles Rouges, Valais)*. *Mémoires de Géologie (Lausanne)* 9, 101 pp.
- PUPIN, J.P. (1980): *Zircon and Granite Petrology*. *Contrib. Mineral. Petrol.* 73, 207–220.
- PUPIN, J.P. (1988): *Granites as indicators in palaeogeodynamics*. *Rend. Soc. Ital. Mineral. Petrol.* 43, 237–262.
- REY, P., BURG, J.P. and CASEY, M. (1997): The Scandinavian Caledonides and their relationship to the Variscan belt. In: BURG, J.P. and FORD, M. (eds): *Orogeny through time*. *Geol. Soc. London Spec. Publ.* 121, 179–200.
- ROLLINSON, H. (1993): *Using geochemical data: evaluation, presentation, interpretation*. Longman Scientific & Technical, 352 pp.
- SCHÄFER, A. (1989): *Variscan molasse in the Saar-Nahe Basin (W-Germany), Upper Carboniferous and Lower Permian*. *Geol. Rundsch.* 78, 499–524.
- SCHALTEGGER, U. and CORFU, F. (1992): *The age and source of Late Hercynian magmatism in the Central*

Alps: evidence from precise U–Pb ages and initial Hf isotopes. *Contrib. Mineral. Petrol.* 111, 329–344.

SCHALTEGGER, U. and CORFU, F. (1995): Late Variscan “Basin and Range” magmatism and tectonics in the Central Alps: evidence from U–Pb geochronology. *Geodinamica Acta* 8, 82–98.

SCHALTEGGER, U. (1997a): The age of an Upper Carboniferous/Lower Permian sedimentary basin and its hinterland as constrained by U–Pb dating of volcanic and detrital zircons (Northern Switzerland). *Schweiz. Mineral. Petrogr. Mitt.* 77, 101–111.

SCHALTEGGER, U. (1997b): Magma pulses in the Central Variscan belt: episodic melt generation and emplacement during lithospheric thinning. *Terra Nova* 9, 242–245.

SCHALTEGGER, U. and BRACK, P. (1999): Short-lived events of extension and volcanism in the Lower Permian of the Southern Alps (Northern Italy, Southern Switzerland). *Terra Nova* 11 (suppl. 1), 296.

SCHULZ, B. and VON RAUMER, J. (1993): Syndeformational uplift of Variscan high-pressure rocks (Col de Bérard, Aiguilles Rouges Massif, Western Alps). *Zeitschr. dt. geol. Ges.* 144, 104–120.

STOLLHOFEN, H. and STANISTREET, G.I. (1994): Interaction between bimodal volcanism, fluvial sedimentation and basin development in the Permo-Carboniferous Saar-Nahe Basin (south-west Germany). *Basin Research* 6, 245–267.

SUBLET, P. (1962): Etude géologique du synclinal Carbonifère de Collonges-Dorénaaz (Valais). *Eclogae geol. Helv.* 55, 23–76.

TAYLOR, S.R. and MCLENNAN, S.M. (1981): The composition and evolution of the continental crust: rare element evidence from sedimentary rocks. *Phil. Trans. R. Soc. A* 301, 381–399.

VON RAUMER, J.F. (1971): Das Mont-Blanc-Massiv – Altkristallin im Bereich schwacher alpiner Metamorphose. *Schweiz. Mineral. Petrogr. Mitt.* 51, 193–225.

VON RAUMER, J.F., MÉNOT, R.P., ABRECHT, J. and BIINO, G. (1993): The Pre-Alpine evolution of the External Massifs. In: VON RAUMER, J.F. and NEUBAUER, F. (eds): *Pre-Mesozoic Geology in the Alps*. Springer Verlag, 221–240.

VON RAUMER, J.F., BUSSY, F. and SHARP, Z. D. (1996): Lac Cornu revisited: the evolution from Lower to Upper Crust (Aiguilles-Rouges Massif, Western Alps). *Schweiz. Mineral. Petrogr. Mitt.* 76, 120–121.

VON RAUMER, J. (1998): The Palaeozoic evolution in the Alps: from Gondwana to Pangea. *Geol. Rundsch.* 87, 407–435.

VON RAUMER, J., ABRECHT, J., BUSSY, F., LOMBARDO, B., MÉNOT, R.-P. and SCHALTEGGER, U. (1999): The Palaeozoic metamorphic evolution of the Alpine External Massifs. *Schweiz. Mineral. Petrogr. Mitt.* 79, 5–22.

VOSHAGE, H., HOFMANN, A.W., MAZZUCHELLI, M., RIVALENTI, G., SINIGOI, S., RACZEK, I. and DEMARCHI, G. (1990): Isotopic evidence from the Ivrea Zone for a hybrid lower crust formed by magmatic underplating. *Nature* 347, 731–736.

WAIKITA, H., REY, P. and SCHMITT, R.A. (1971): Abundances of the 14 rare-earth elements and 12 other trace elements in Apollo 12 samples: five igneous and one breccia rocks and four soils. *Proc. 2nd lunar Sci. Conf.*, Pergamon Press Oxford, 1319–1329.

WASSERBURG, G.J., JACOBSEN, S.B., DEPAOLO, D.J., MCCULLOCH, M.T. and WEN, T. (1981): Precise determination of Sm/Nd ratios, Sm and Nd isotopic abundances in standard solutions. *Geochim. Cosmochim. Acta* 45, 2311–2323.

WEIL, M. (1999): Die Geologie der Montagne Fully, im Bereich des Lac de Fully (Wallis, Westschweiz). Unpubl. Diploma Thesis, Univ. Freiburg i. Br., 82 pp.

WINCHESTER, J.A. and FLOYD, P.A. (1977): Geochemical discrimination of different magma series and their differentiation products using immobile elements. *Chem. Geol.* 20, 325–343.

ZIEGLER, P.A. (1990): Geological Atlas of Western and Central Europe (second and completely revised edition). Shell Internat. Petroleum Maatschappij BV, The Hague, 239 pp.

ZIEGLER, P.A. (1993) Late Palaeozoic – Early Mesozoic plate reorganization: evolution and demise of the Variscan fold belt. In: VON RAUMER, J.F. and NEUBAUER, F. (eds): *Pre-Mesozoic Geology in the Alps*. Springer Verlag, 203–216.

Manuscript received January 3, 2000; revision accepted May 26, 2000.

Annex 1 Short description and location of the investigated samples.

Samples	Macroscopic description	Coordinates*
CN 125	subaerial basal flow (SD)	570065/113798
CN 252/b	rhyolitic pebble (SD)	564430/101180
CN 252/d	rhyolitic pebble (SD)	564430/101180
CN 118	tuff layer (SD)	573222/114295
CN 121	tuff layer (SD)	573895/113252
CN 122	tuff layer (SD)	573895/113252
CN 256	tuff layer (SD)	564465/100895
CN 256a	tuff layer (SD)	564465/100895
CN 257	tuff layer (SD)	564440/100405
CN 257a	tuff layer (SD)	564440/100405
CN 108	Volcaniclastic layer (SD)	572485/112500
CN 113	Volcaniclastic layer (SD)	572935/112038
CN 140	Volcaniclastic layer (SD)	572590/114300
FB 947	MB rhyolite	572000/085300
MR2809	MB rhyolite	574495/102915
BR1466	AR rhyolite	563575/108660
FB 803	MB granite	569175/095665

* Coordinates refer to 1:25'000 Swiss National topographic maps.